VOLUME 29 MAY, 1951 NUMBER 3

Canadian Journal of Physics

Editor: G. M. VOLKOFF

Published by THE NATIONAL RESEARCH COUNCIL
OTTAWA CANADA

CANADIAN JOURNAL OF PHYSICS

This was formerly *Section A, Canadian Journal of Research.* The change to the new name took place January 1, 1951. The CANADIAN JOURNAL OF PHYSICS is published six times annually.

The CANADIAN JOURNAL OF PHYSICS is published by the National Research Council of Canada under the authority of the Chairman of the Committee of the Privy Council on Scientific and Industrial Research. Matters of general policy are the responsibility of a joint Editorial Board consisting of members of the National Research Council of Canada and the Royal Society of Canada.

The National Research Council of Canada publishes also the following Journals: *Canadian Journal of Botany, Canadian Journal of Chemistry, Canadian Journal of Medical Sciences, Canadian Journal of Technology, Canadian Journal of Zoology.*

EDITORIAL BOARD

Representing
NATIONAL RESEARCH COUNCIL

*DR. H. P. ARMES (*Chairman*),
Emeritus Dean of Arts and Science,
University of Manitoba,
Winnipeg, Man.

DR. OTTO MAASS,
Macdonald Professor of Physical Chemistry,
McGill University,
Montreal, P.Q.

DR. J. H. L. JOHNSTONE,
Professor of Physics,
Dalhousie University,
Halifax, N.S.

DR. A. BERTRAND,
Professor of Bacteriology,
Faculty of Medicine,
University of Montreal,
Montreal, P.Q.

Representing
ROYAL SOCIETY OF CANADA

DR. G. M. VOLKOFF,
Professor of Physics,
University of British Columbia,
Vancouver, B.C.

DR. J. W. T. SPINKS,
Dean, College of Graduate Studies,
University of Saskatchewan,
Saskatoon, Sask.

Section III

DR. H. S. JACKSON,
Head, Department of Botany,
University of Toronto,
Toronto, Ont.

DR. E. HORNE CRAIGIE,
Department of Zoology,
University of Toronto,
Toronto, Ont.

Section V

Ex officio

DR. LÉO MARION, *Editorial Adviser*,
Division of Chemistry,
National Research Laboratories,
Ottawa.

DR. H. H. SAUNDERSON,
Director, Division of Information Services,
National Research Council,
Ottawa.

Representing
THE CHEMICAL INSTITUTE OF CANADA

DR. H. G. THODE,
Department of Chemistry,
McMaster University,
Hamilton, Ont.

Subscription rate: $2.00 a year. All enquiries concerning subscriptions should be addressed to the CANADIAN JOURNAL OF PHYSICS, National Research Council, Ottawa, Canada. Special rates can be obtained for subscriptions to more than one of the Journals published by the National Research Council.

*Deceased.

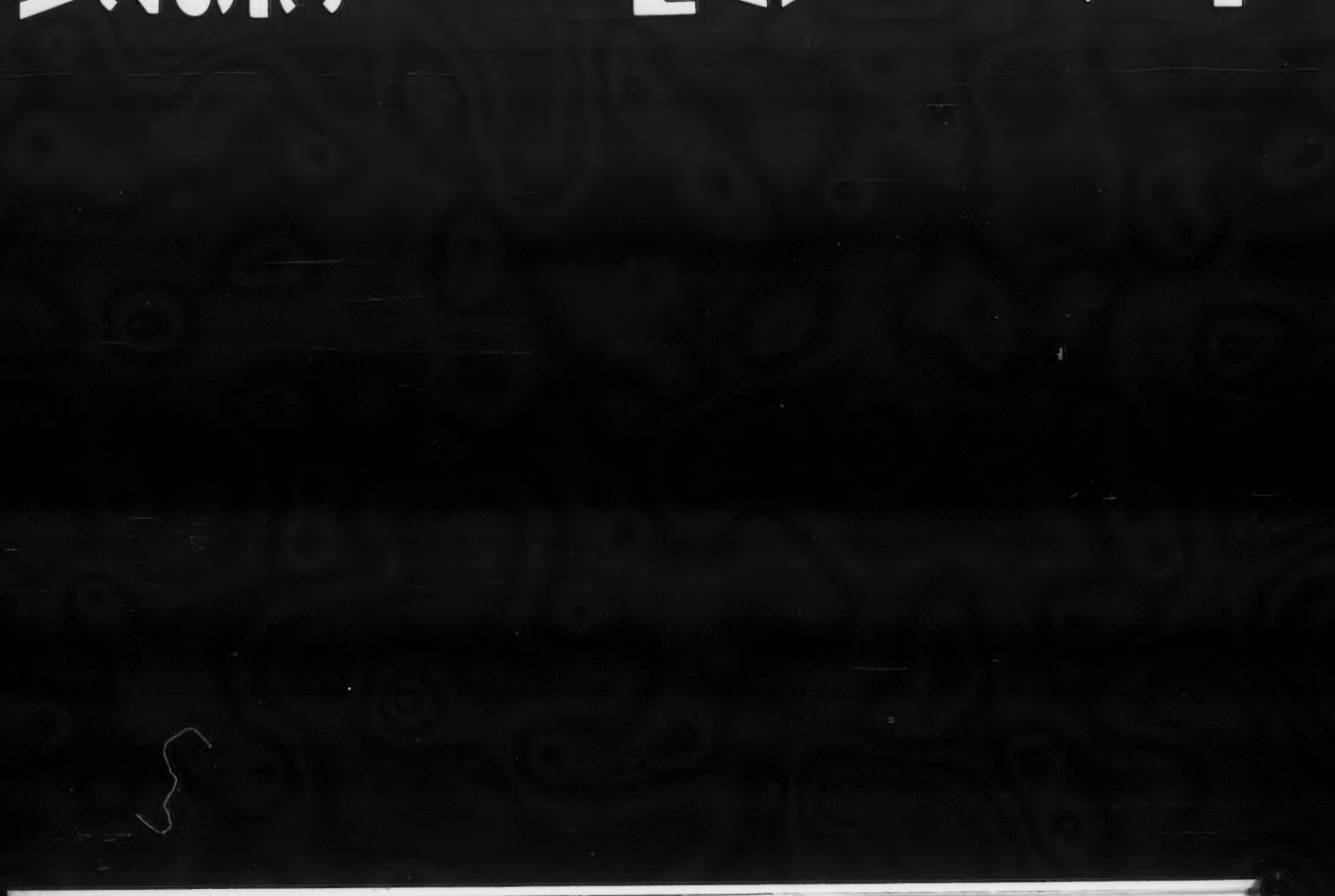

Canadian Journal of Physics

Issued by THE NATIONAL RESEARCH COUNCIL OF CANADA

VOLUME 29 MAY, 1951 NUMBER 3

ON THE PENETRATING SHOWERS OF COSMIC RAYS[1]

BY ANDRÉ G. VOISIN[2]

Abstract

Experiments have been carried out at sea level to measure penetration of particles from local showers produced in lead as a function of the angular width of the cone of shower particles. The shower particles are assumed to be mesons and are observed by counter arrangements connected in coincidence and anticoincidence.

The results show that the showers containing the more penetrating particles are those of wide angular spread. The multiplicity of penetrating particles per shower is estimated to be at least 3.7, and the curve of the angular distribution shows a maximum corresponding to a shower cone of a half angle of about 15°.

I. Introduction

In photographic plate studies at high altitudes, stars which include a group of minimum ionization particles (1, 5, 11, 15, 16) are often found. The group of energetic particles usually follows the same general direction as the primary particles and it is becoming accepted that a large portion of these particles are mesons (1, 22). Similar showers of penetrating particles have been found in Wilson expansion chamber tracks (for example: 3, 8) and have been identified by W. B. Fretter (4) as a mixture of protons and mesons. The mesons are π mesons as they are produced locally (19). Lewis, Oppenheimer, and Wouthuysen (13, 14) point out the importance of knowing the multiplicity and the angular distribution of mesons produced by a single primary. This, with a knowledge of the energy of the primary, would obviously be of great assistance in selecting the best of various meson theories.

The measurements described here are an attempt to observe the behavior of local penetrating showers as a function of their lateral spread.

II. Experimental Arrangement

The experiments were carried out at sea level in Ottawa by means of counters and lead absorbers arranged as shown in Fig. 1. The counters were of the metal type, similar to those which have already been described (12), 2.5 cm. in diameter and 40 cm. in length. Counters 1, 2, 3, 4, 5 were connected in fivefold coincidence, and the group controlled a master circuit (20, 21) in such a way that the remaining counter pulses would not be recorded unless an

[1] *Manuscript received December 4, 1950.*
Contribution from the Division of Physics, National Research Laboratories, Ottawa. Issued as N. R. C. No. 2357.

[2] *Attaché de recherches au Centre National de la Recherche Scientifique, Paris. Holder of a National Research Council of Canada postdoctorate fellowship.*

impulse from this fivefold coincidence occurred to make the circuit sensitive. These fivefold coincidences are designated as M.

Each of the analyzer-counters A_1, A_2, B_1, B_2, C_1, C_2, and each group of counters K_1, K_2, L and S, were connected individually in coincidence with M and the pulses were recorded separately by means of a multiple pen recorder. The thickness of the lead absorber P_1 was varied between 0 and 35 cm. The absorbers P_2 and P_3 were each only 5 cm. thick so as to permit the recording of penetrating showers, which are significantly softer than those generally studied. The absorbers Q_1 and Q_2 were each 5 cm. thick and the counter groups K and L with their absorbers give the relative penetration of showers of different angular spreads which are indicated by the counters discharged in the row of analyzer counters J.

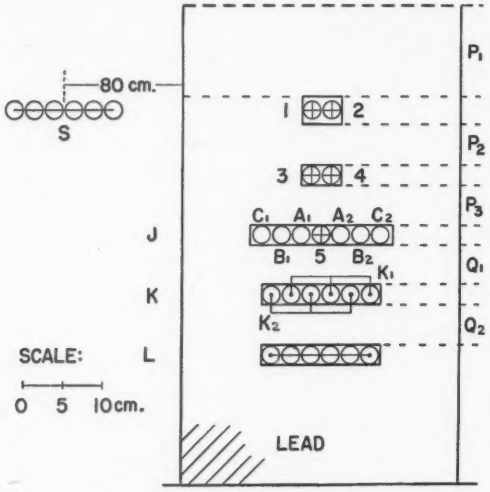

FIG. 1. *Schematic diagram of counters and lead absorbers.*

An exact measure of the angular width is not possible because the geometry does not indicate the point in the absorber P_1 where a shower originated. For very large showers some of the most divergent particles would also be missed. The shower telescope does not indicate the direction of the primary particle which produced the shower. However, it was mounted vertically and the symmetry of the arrangement of counters was such that the observed showers would be mainly in a vertical direction. The number of counters discharged in the analyzer group gives an indication of the multiplicity of penetrating particles in the shower. The resolving time of the counter circuits was sufficiently short that accidental coincidences are negligible.

Knock-on Electrons Produced by Mesons

A single meson crossing the apparatus could be mistaken for a shower if it produced multiple knock-on electrons. Two such electrons from a meson

could cause a fivefold coincidence M or three could be recorded as a shower discharging M plus one counter in J. An estimate of the maximum possible number of double knock-on events can be made by assuming that *all* the fivefold coincidences M are due to double knock-on when no counters J are discharged simultaneously (anticoincidences M-J). The counting rate of the anticoincidences M-J is 0.5 per hour; this value is considered to be an upper limit for the number of double knock-on events.

Triple knock-on events can be estimated by connecting the counters 1 to 5 as three units: (1, 2) in parallel, (3, 4) in parallel, and 5 alone and recording triple coincidences. The triple coincidences represent the number of single mesons passing through the telescope. This triple coincidence group in coincidence with one counter in the J row gives the probability of a meson coming out of absorber P_3 accompanied by a knock-on electron. The meson rate was 675 per hour and 6% of these were accompanied by at least one particle detected in the J counters. This is in agreement with the results of Brown *et al.* (2) who found 7% of knock-on secondary particles under half inch of lead.

It can be assumed therefore that 6% of the double knock-on events, represented by the M-J rate, or 0.03 per hour is the maximum number of triple knock-on events that could be recorded by M plus at least one counter in J (coincidence $M.J \geqslant 1$ counter). Therefore, the frequency of the false coincidences induced by triple knock-on events is low compared with the $M.J \geqslant 1$

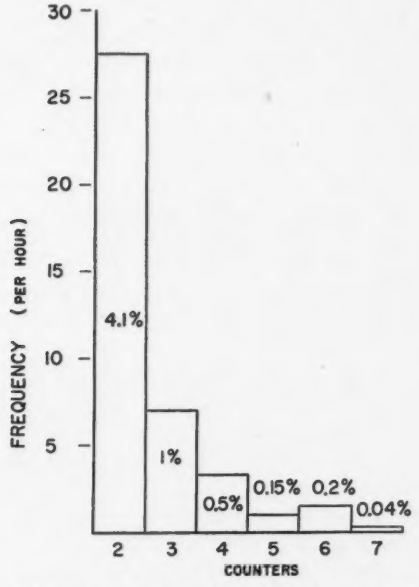

FIG. 2. *Angular distribution of secondaries from single mesons.*

coincidence rate, which is about 0.5 per hour. To exclude errors due to double knock-on, only the coincidences $M.J \geqslant 1$ are used.

The lateral spread of the secondaries from single mesons can be deduced from the above measurements, wherein counters 1 to 5 were connected in triple coincidence $(1+2).(3+4).5$ and coincidences recorded between those and each of the analyzer counters in row J. Fig. 2 shows the lateral spread of secondary particles accompanying mesons, the abscissa representing the lateral spread indicated by the extreme counters discharged in row J. This figure shows that the secondary particles produced by a single meson have a trajectory that is rarely very divergent from that of the incident meson. This had already been noticed by Brown *et al.* (2) who find that the secondaries produced by the mesons of $E > 200$ Mev. are distributed according to a law of $\cos^{2.5}\alpha$, α being the angle between the two trajectories. On the other hand the present results show that for 161 recorded events, 226 counters were discharged in the J row, which gives a lower limit of $226/161 = 1.4$ secondary particles accompanying a meson. The majority of these showers discharged only one counter in row J, but sometimes 4, 5, and even 6 counters were discharged.

III. Experimental Results

The frequency of the showers discharging the five counters M and at least one of the J counters (coincidences $M.J \geqslant 1$) were recorded as a function of the thickness of the absorber P_1 which was varied between 0 and 35 cm. of lead. The observed rates are shown in Table I and are represented by curves in Fig. 3. Integral curve (a) shows the number of showers with range greater than 10 cm. of lead and integral curve (b) the showers of range greater than 20 cm. of lead, i.e., of the showers recorded by the coincidences $M.J \geqslant 1.K.L$ in which at least one particle reached the levels K and L. The curves obtained

TABLE I

Thickness of P_1 in cm. lead	0	5	20	35
Rate per hour of the showers of range $>$ 10 cm.	0.450±0.039	0.517±0.053	0.610±0.053	0.467±0.036
Rate per hour of the showers of range $>$ 15 cm.	0.264±0.030	0.441±0.049	0.489±0.047	0.398±0.034
Rate per hour of the showers of range $>$ 20 cm.	0.190±0.026	0.322±0.042	0.418±0.043	0.329±0.030

have a shape approximately similar to the transition curve obtained in lead by Jánossy and Rochester (9) and shows a slight maximum near 20 cm. of lead in P_1. However, taking into account the area of the counters, the observed counting rates in curve (a) are higher than those given by other authors (10). This shows that these measurements include rather more than the showers usually classed as penetrating showers. For $P_1 = 0$ and probably for $P_1 = 5$ cm. of lead a high counting rate would be expected because the results include an appreciable number of energetic cascade electron showers. This was also shown by making measurements with $P_1 = 2$ cm. With this

thickness of lead the Rossi maximum appears, the integral rate being 0.75 shower per hour. As noted before, the softest showers observed must go through at least 10 cm. of lead, and only electrons of an energy greater than 10^4 Mev. have a measureable chance of going through this thickness of absorber.

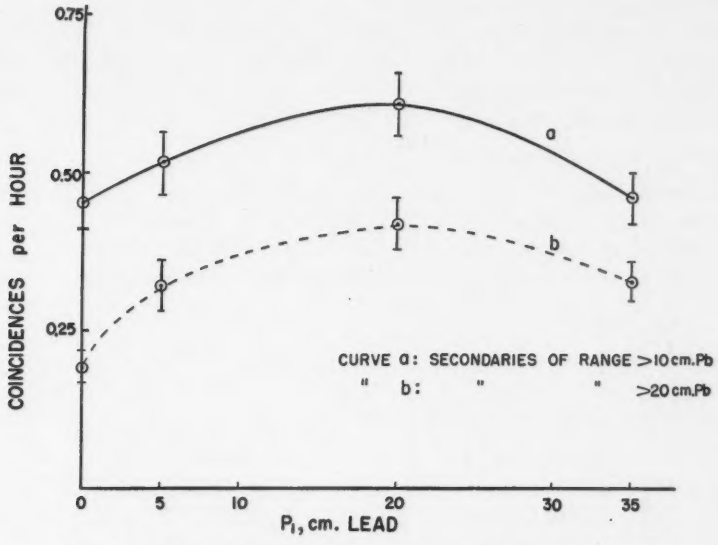

FIG. 3. *Frequency of the showers vs. the thickness of the upper absorber* P_1.

If $P_1 = 20$ cm., which makes $P_1 + P_2 + P_3 = 30$ cm. of lead or about 60 cascade units, it would be necessary to start with a primary electron of 10^{10} Mev. to penetrate these absorbers. The number of electrons with energies of this order is much too small to explain the observed rates (6). A fortiori for $P_1 = 35$ cm. of lead, the cascade energy would be of the order of 10^{12} Mev. Therefore the recorded showers under 20 and 35 cm. of lead are probably not cascade showers, unless they are due to the electron component in equilibrium with meson component. Such cascades might originate from radiative collision of mesons, from meson decay in flight, or from knock-on electrons. But it is obvious that the first and second possibilities are not very likely since the probability of radiative collision of a meson is very small and the probability of high energy meson decay in flight taking place in the apparatus is negligible.

Triple knock-on electrons which would be recorded as showers have been discussed in previous paragraphs. The frequency of these was estimated to be about 6% of the recorded showers and these would only be mostly within two counter widths of the axis defined by the M group.

An estimate of the number of air showers (Auger showers) was made by the use of an additional tray of counters S (Fig. 1). This tray had an area of 600 cm.^{2} and was placed at a distance of 80 cm. to one side of the main telescope. The rate in coincidence with M was found to be 0.08 $\pm$ 0.03 per hour. This rate therefore is low and one can conclude that the contribution of counts due to air showers is small.

In conclusion it seems reasonable to assume that, though the showers studied in this experiment include somewhat softer showers than those ordinarily termed "penetrating showers", the number of cascade electron showers included is very small with $P_1 = 20$ and 35 cm. of lead and the remainder are penetrating showers produced in the lead absorber P_1.

Penetration of Shower Particles

The penetration of the showers can be shown by the number of showers able to reach the row of counters K and L separated by the absorbers Q_1 and Q_2. In the experiments described here the counters of each row K_1 and K_2 were connected in parallel and it takes only one particle to activate them.

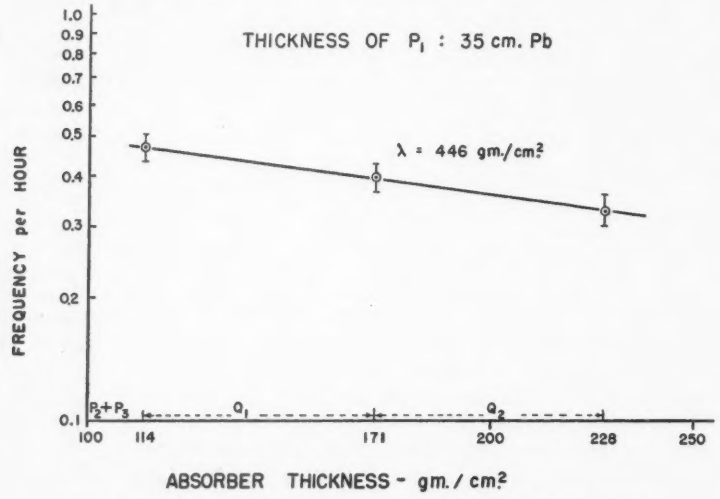

FIG. 4. *Absorption of the secondary particles with $P_1 = 35$ cm. of lead.*

The results are shown in Fig. 4, wherein the relative counting rates are plotted in a logarithmic scale against the thickness of the lower absorbers. The three plotted points represent coincidences $M.J$, coincidences $M.J.K$, and coincidences $M.J.K.L$. The points fall on a straight line. Similar curves for different thicknesses of P_1 also show points falling on a straight line indicating that the probability of penetrating particles reaching different depths in lead absorbers is an exponential function. The mean range as deduced from

the slope of curve like Fig. 4 is plotted in Fig. 5 as a function of the thickness of absorber P_1. Though the energy of the shower particles is not known, Fig. 5 shows the expected result that more penetrating showers are observed with increasing thickness of P_1.

As shown in Part II the penetration can be studied as a function of the lateral spread of the showers by observing the coincidences in K and L in relation to the position of the extreme counters in row J which are discharged. The lateral spread is given by the position of the counters discharged in row J but as the direction of the center of the shower is not indicated by M, no consideration was given to symmetry about telescope M. In Tables II, III, and IV and in Fig. 5 the lateral spread is indicated by the distance in counter

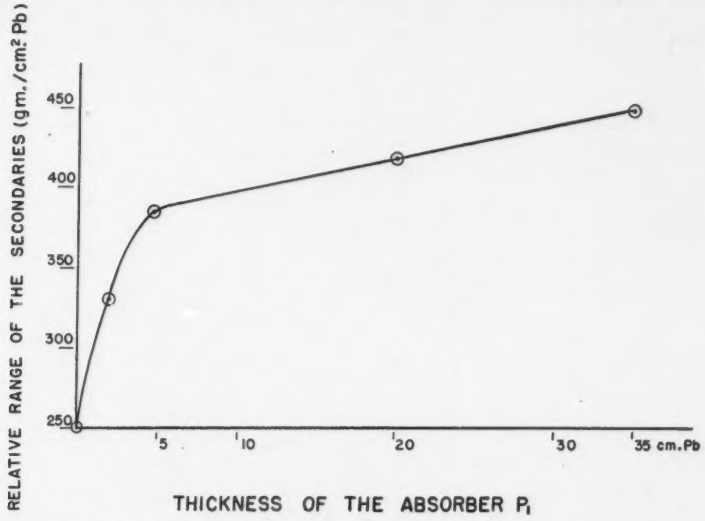

FIG. 5. *Relative range of the showers vs. the thickness of absorber* P_1.

widths between extreme counters discharged (including the counters discharged). Lateral spreads of 1 were excluded as explained above in order to eliminate any appreciable effect due to knock-on electrons. Table II shows the frequency of the showers as a function of their lateral spread.

Table III indicates the frequency of the showers stopped in absorbers Q_1 and Q_2 for different lateral spreads. In Fig. 6 the ordinates are subdivided to show the number of showers, from which at least one particle would reach counters K or L. Table IV deduced from Table III shows the ratio of the number of showers stopped in absorbers Q_1 and Q_2 to the number of showers not stopped. Fig. 7 indicates the relative range of the showers as a function of their lateral spread. The range is calculated according to an exponential absorption by the method indicated above and is not an absolute measurement.

TABLE II

Lateral spread (in number of counters)	2	3	4	5	6	7
Frequency of the showers per hour	0.082±0.014	0.104±0.017	0.112±0.018	0.061±0.013	0.039±0.010	0.069±0.014

TABLE III

Lateral spread	2	3	4	5	6	7
Stopped in Q_1 per hour	0.022	0.026	0.022			
Stopped in Q_2 per hour	0.017	0.017	0.013	0.013	0.009	

TABLE IV

Lateral spread	2	3	4	5	6
$\frac{\text{Stopped in } Q_1 + Q_2}{\text{Total rate}} \times 100$	48%	41%	31%	21%	23%

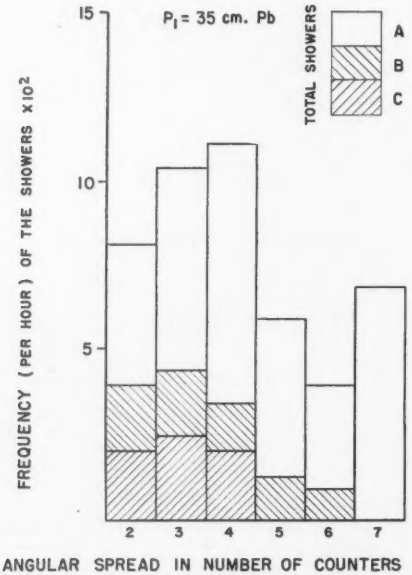

FIG. 6. *Frequency of the showers as a function of their angular spread. A represents the showers not stopped in the absorber $Q_1 + Q_2$; B represents the showers stopped in Q_2; and C represents the showers stopped in Q_1.*

We can see from these experimental data that in the case of large lateral spread almost all the showers go through the absorbers Q_1 and Q_2, whereas about 50% of the narrowest showers (spread 2 or 3) are stopped in the same absorbers. In other words, *the most penetrating showers are the most divergent.* These results, though rather unexpected, are not in contradiction with the calculations of C. Peyrou, B. d'Espagnat et L. Leprince-Ringuet (17, 18). These calculations indicate that the probability for the emission of a meson very divergent from the direction of the primary, in the laboratory reference system, is greater with the more energetic primaries. In the case of a *meson shower of a given number of mesons* the shower will be more divergent the

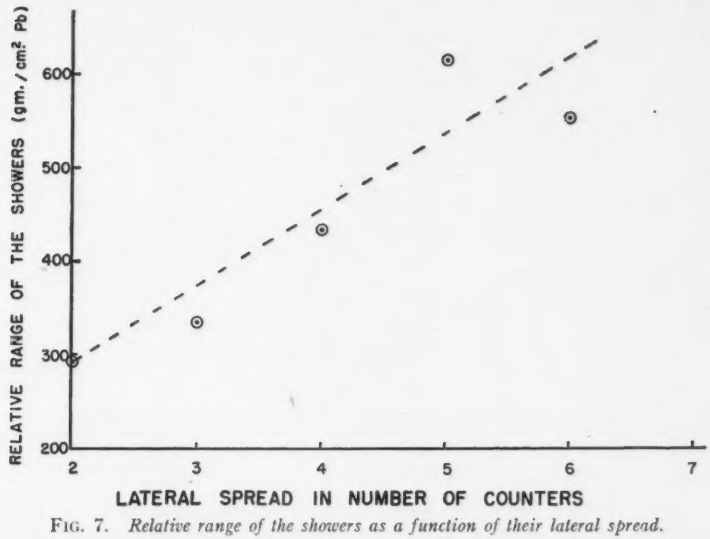

FIG. 7. *Relative range of the showers as a function of their lateral spread.*

greater the energy of the primary. It is assumed that the mesons are created at one time, that is, implicitly according to a multiple production process. As far as they are in agreement with the calculations mentioned above (in particular if the multiplicity does not increase rapidly with the energy of primaries) the experimental results described here favor a multiple production process in regard to mesons produced at sea level in the local penetrating showers.

Angular Distribution

Though the experiments were not designed specifically to study the angular distribution, some information on this can be obtained if the results are treated correctly. Fig. 6 shows the lateral spread of showers in units of counter widths as described above. If the origin of the shower were known the lateral spread would be indicated by the angle of the cone containing the mesons, this solid

angle being projected on a plane perpendicular at the axis of the counters. The telescope M does not indicate the origin of the shower but it is assumed that the showers are produced at an average distance of 5 cm. from the top of absorber P_1. This distance corresponds to a cross section for the production of penetrating showers by a primary nucleon of the same order as the geometrical cross section of the nucleus (7, 23, 25). Most of the primary particles producing showers will be vertical, as W. D. Walker (24) has shown that the distribution of primaries at sea level is strongly dependent on the zenith angle. In these experiments therefore the primary direction can be considered to be the axis of telescope M.

There are two maxima in Fig. 6, the first at the lateral spread of three counters and the second at the lateral spread of seven counters. Their presence cannot be explained by statistical fluctuations even though these are large for any one curve. The two maxima appear for several values of P_1 though only the curve for $P_1 = 35$ cm. is shown. The geometry of the counters was carefully studied in calculating the various probabilities to record the showers of 2, 3, . . . n particles for various origins of these showers. From this study a sensitivity curve was derived for the apparatus, which shows a collimation effect for the group of five counters M. When corrections are made for this, it appears that the first maximum corresponding at the lateral spread of three counters is very likely due to the geometrical arrangement of the counters, but the second maximum at a lateral spread of seven counters is certainly real. For the purpose of determining its position with more accuracy two complementary experiments were carried out.

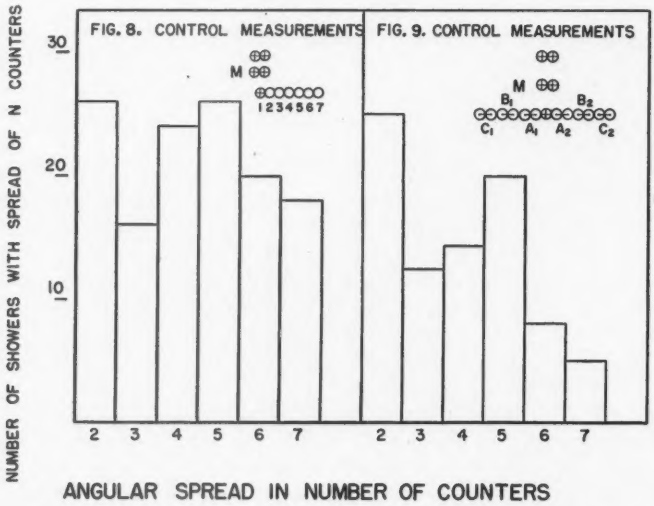

FIG. 8 *and* 9. *Control measurements of the shower rate vs. their lateral spread.*

In the first experiment, instead of placing the analyzing counters J symmetrically with respect to the group of five counters M, six counters in row J were placed all on one side of M. Fig. 8 shows the resulting curve for $P_1 = 35$ cm. of lead. To improve the statistics a second experiment was carried out wherein counters were used in groups of two (in parallel), three groups on each of the center counter five. Fig. 9 obtained with this arrangement and Fig. 8 both show a maximum at five counters, the maximum at two being instrumental as explained before. The altered geometry of the arrangement in comparison with the original arrangement displaces the maxima to the left.

From the position of this second maximum and the assumption that the average level of production in the absorber is 5 cm. from the top, the angular width of the cone of particles at this maximum is estimated to be of the order of 30°. (The projected angle was multiplied by $\sqrt{2}$ in order to obtain the true angle.) These results indicate the possibility of a maximum in the number of shower particles making an angle of 15° with the primary.

Multiplicity

Each of the counters of tray J subtends an angle of about 3° when $P_1 = 35$ cm. of lead. The probability for one counter to be struck by several particles of the same shower is low, except in the case of very dense showers. The observed average number of particles is a minimum for this reason and also because the particles greatly displaced from the core of the shower are missed. The results indicate an average number of 3.7 particles per shower, which seems to indicate that the showers are pretty well grouped in the forward direction as this number agrees roughly with that found by other methods. For instance, an average of four particles is found by cloud chamber measurements.

IV. Conclusions

The experiments described here were carried out at sea level on the showers of range greater than 10 cm. of lead. Special care was taken to eliminate the knock-on electrons from the single mesons. The showers were produced in a lead block placed just above the counters.

The results indicate that the showers selected are more penetrating with increasing lateral spread. On the average they have at least 3.7 penetrating particles per shower contained in a cone of half angle of the order of 15°. The results suggest that local penetrating showers could be produced at sea level by a "multiple" process. With a view to testing this assumption, further observations are considered desirable.

Acknowledgments

I wish to thank Prof. A. Dauvillier and Dr. A. Rogozinski for their active encouragement and Dr. J. Pirenne for helpful discussions. I particularly wish to thank Dr. D. C. Rose for his generous aid in the analysis and presentation of the data and for his many constructive suggestions.

References

1. BROWN, R., CAMERINI, U., FOWLER, P. H., MUIRHEAD, J., POWELL, C. F., and RITSON D. M. Nature, 163: 47. 1949.
2. BROWN, W. W., MCKAY, A. S., and PALMATIER, E. D. Phys. Rev. 76: 506. 1949.
3. DAUDIN, J. Ann. phys. Paris, 19 (11): 110. 1941.
4. FRETTER, W. B. Phys. Rev. 76: 511. 1949.
5. HORNBOSTEL, J. and SALANT, E. O. Phys. Rev. 76: 468. 1949.
6. JÁNOSSY, L. Cosmic rays. Oxford University Press, 1950. p. 351.
7. JÁNOSSY, L. and BROADBENT, D. Nature, 155: 142. 1945.
8. JÁNOSSY, L., MCCUSKER, C. B. A., and ROCHESTER, G. D. Nature, 148: 660. 1941.
9. JÁNOSSY, L. and ROCHESTER, G. D. Proc. Roy. Soc. A, 182: 180. 1943.
10. JÁNOSSY, L. and ROCHESTER, G. D. Proc. Roy. Soc. A, 183: 181. 1944.
11. LEPRINCE-RINGUET, L., BOUSSER, F., HOANG-TCHANG-FONG, JAUNEAU, L., and MORELLET, D. Compt. rend. 229:163. 1949.
12. LESAGE, M., ROGOZINSKI, A., and VOISIN, A. J. phys. 10: 212. 1949.
13. LEWIS, H. W. Phys. Rev. 76: 566. 1949.
14. LEWIS, H. W., OPPENHEIMER, J. R., and WOUTHUYSEN, S. A. Phys. Rev. 73: 127. 1949.
15. LORD, J. J. and SCHEIN, M. Phys. Rev. 77: 19. 1950.
16. PETERS, B., BRADT, H., and KAPLON, M. Phys. Rev. 76: 1735. 1949.
17. PEYROU, C. and D'ESPAGNAT, B. Compt. rend. 228: 674. 1949.
18. PEYROU, C., D'ESPAGNAT, B., and LEPRINCE-RINGUET, L. Compt. rend. 228: 1777. 1949.
19. PICCIONI, O. Phys. Rev. 77: 1. 1950.
20. REGENER, E. Phys. Rev. 64: 252. 1943.
21. ROGOZINSKI, A. Thèse doctorat ès Sc. Paris, 1945.
22. ROSSI, B. Revs. Modern Phys. 20: 537. 1948.
23. SCHEIN, M., IONA, M., and TABIN, J. Phys. Rev. 64: 253. 1943.
24. WALKER, W. D. Phys. Rev. 77: 686. 1950.
25. WATAGHIN, G. Nature, 161: 91. 1948.

SELECTIVE REFLECTION FROM THE VAPORS OF THE ALKALI METALS[1]

By A. C. Lauriston[2] and H. L. Welsh

Abstract

Selective reflection from sodium, potassium, rubidium, and caesium vapors in the neighborhood of the resonance lines was observed for vapor pressures between 10 mm. and 1 atm., using a steel tube with a window of transparent magnesium oxide. Reflecting power as a function of frequency was measured by using incident light of continuous spectral distribution. The reflection contour for pressures up to 1/2 atm. is in good agreement with the theory of reflection from an absorbing medium. For each line the damping constant in the dispersion equations varies as the square root of the number of atoms per cubic centimeter, as was found previously for mercury and cadmium. For the two members of the resonance doublet the damping constants are proportional to the square roots of the oscillator strengths. In a region about 5 cm.$^{-1}$ wide about each resonance frequency the reflected intensity measured experimentally is greater than that calculated. These lines of residual intensity may be due to a second kind of selective reflection. At pressures above 1/2 atm. the observed reflection contour cannot be explained by the simple anomalous dispersion theory.

Introduction

Selective reflection from metallic vapors in the neighborhood of resonance lines, discovered by Wood (11) for the mercury line at 2537Å, has been shown recently by Welsh, Kastner, and Lauriston (10) to be in general quantitative agreement with the classical theory of reflection from an absorbing medium. In these experiments the variation of reflecting power with frequency was determined by intensity measurements in a continuum reflected from a quartz-metallic vapor interface. Experimental reflection contours in the region of Hg 2537Å and Cd 2288Å were fitted by calculated intensity distributions obtained by varying the values of the oscillator strength, f, and the damping constant, γ, in the anomalous dispersion equations. This procedure was carried out for a series of vapor pressures of the metals. The oscillator strength of each line was independent of the pressure and in agreement with values obtained by other methods. The damping constant was found to be proportional to the square root of the number of atoms per cubic centimeter, indicating that the mechanism of selective reflection is essentially different from that of absorption and emission. For cadmium vapor at low pressures a line of residual intensity was left at the resonance frequency when the calculated contour giving the best over-all fit was subtracted from the experimental contour. At pressures above 5 atm. it was not possible to obtain a calculated contour in agreement with experiment by variation of the oscillator strength and damping constant.

In the present investigation selective reflection was observed for the resonance lines of the alkali metals, sodium, potassium, rubidium, and caesium.

[1] *Manuscript received November 10, 1950.*
Contribution from the McLennan Laboratory, University of Toronto, Toronto, Ontario.

[2] *Holder of the E. F. Burton Fellowship in Physics, School of Graduate Studies, University of Toronto, 1948-50. Now in the Operational Research Group, Defence Research Board, Ottawa, Canada.*

These lines, due to the transitions $^2S_{1/2} - {}^2P_{1/2,3/2}$, are doublets with separations varying from 17.2 cm.$^{-1}$ for sodium to 554 cm.$^{-1}$ for caesium. For the smaller doublet separations the two resonance frequencies had to be taken into account simultaneously in the interpretation of the data. The results obtained confirm generally the conclusions reached for mercury and cadmium, and, in addition, show new empirical relationships connecting the damping constant with the oscillator strength and frequency of the line.

Experimental Procedure

At high temperatures the vapors of the alkali metals attack quartz and glass, causing them to blacken rapidly. However, Strong and Brice (1, 9) have shown that transparent magnesium oxide (optical periclase) is not affected by the alkali metals, and that it is possible to construct steel cells with windows of this material, which remain vacuum-tight on heating to high temperatures.

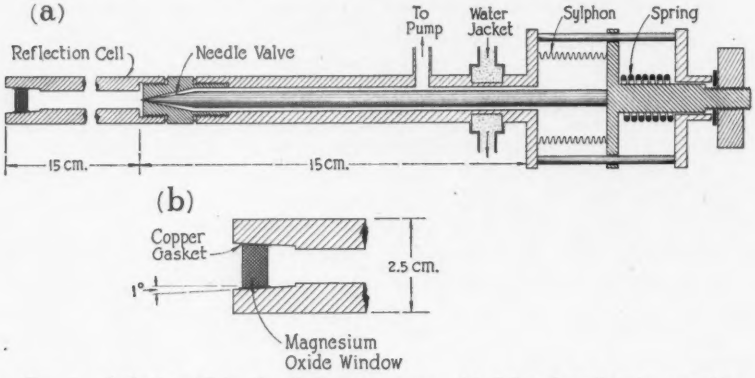

FIG. 1. *Reflection cell for the alkali metal vapors. (a) Cell and needle valve assembly. (b) Detail of the window mount.*

The reflection cell (Fig. 1) was a steel tube closed at one end with a magnesium oxide* window sealed with a copper gasket, and fitted at the other end with a needle-valve assembly. Considerable care was required to produce a good seal between the window and the steel tube. A magnesium oxide disc about 10 mm. in diameter and 5 mm. thick, with its plane surfaces polished to form a prism of small angle, was ground and polished in a steel cone of 1° taper until a uniform finish was obtained around the circumference of the disc. The window was then lapped in contact with a thin conical copper gasket, which in turn was lapped in the conical opening at the end of the steel cell (Fig. 1*b*). The surfaces in contact were thoroughly cleaned before the window and gasket were finally pressed into position in the cell. Seals formed in this manner were tight on heating up to 750–800°C. but did not always remain tight on cooling from high temperatures.

**The authors are indebted to Norton Company, Niagara Falls, Canada, who furnished the magnesium oxide crystals used in this investigation.*

Another, much simpler, method of sealing was successful for temperatures up to 500°C. The bore of the steel tube was enlarged to form a recess into which the circular window disc fitted loosely. The recess in the tube was coated with a silver solder of low melting point and the window was inserted. The tube was then heated with a torch until the solder melted and flowed around the window. The magnesium oxide did not fracture on cooling and the seal was very strong mechanically. Unfortunately, this type of seal could not be used in this investigation since, with alkali metal vapors present, the solder melted at about 500°C., a hundred degrees below its normal melting point.

Commercial grade sodium and potassium were heated in vacuum to remove the oil and then washed in ether. The metal, still covered with ether to prevent oxidation, was introduced through the open end of the cell into which the needle-valve assembly was screwed. Rubidium and caesium were prepared in vacuum by reduction of the chloride with calcium filings, and distilled into glass capsules which were sealed. The capsule containing the metal was broken in an atmosphere of argon and inserted into the cell which had been flushed with argon. After the needle valve was attached the cell was evacuated and then sealed by closing the valve.

The cell was heated in a differentially wound platinum furnace which extended from about 5 cm. in front of the window to a point near the outlet to the vacuum pump (Fig. 1*a*). To prevent condensation of vapor on the window it was necessary to maintain a temperature difference of about 50°C. between thermocouples mounted on the cell near the window and near the needle valve. The size of the temperature difference indicates that the temperatures measured were not those prevailing inside the cell.

Light from a tungsten filament lamp was condensed on the window of the cell by a lens which formed an image of the source a few centimeters in front of the window. A second lens collected the light reflected from the inner surface of the window and formed an image of the source on the slit of the spectrograph. Because of the prismatic form of the window light reflected from the outer surface did not enter the spectrograph. Since the resonance lines of the alkali metals occur in the visible and near infrared regions a Hilger E-1 glass spectrograph was used. The reciprocal linear dispersion was 46 $cm.^{-1}$ per mm. in the region of the sodium resonance lines and 61 $cm.^{-1}$ per mm. in the region of the potassium and rubidium resonance lines. The reflected continuum was photographed in 5 to 10 min. on Ilford Long Range Spectrum plates using a spectral slit width of 1 $cm.^{-1}$ for sodium and 2 $cm.^{-1}$ for potassium and rubidium. Each plate was calibrated for intensity measurement by photographing, with the same exposure time, the spectrum of the tungsten lamp with a stepped slit replacing the usual spectrograph slit. For frequency calibration the spectrum of an Osram caesium lamp was photographed in juxtaposition with each spectrum of the reflected continuum. The potassium and rubidium reflection contours were calibrated with respect to the resonance lines of these metals which were present as impurities in the caesium lamp. The sodium reflection spectra

were calibrated with respect to a weak caesium line at 5844.7Å. The absolute accuracy of the calibration was about 1 cm.$^{-1}$.

Experimental Results

Selective reflection corresponding to both resonance lines of sodium, potassium, rubidium, and caesium was observed. The vapor pressure for the first appearance of the anomalous reflection was about 10 mm. in each case. This agrees with the empirical rule, deduced from the results on mercury and cadmium (10), that with increasing vapor density selective reflection first appears when the product of the oscillator strength of the line and the number of atoms per cubic centimeter reaches a value which is constant for a given experimental arrangement. The value of the constant depends on the resolving power of the detecting apparatus; for the quartz and glass spectrographs used in these experiments the value of Nf for the first appearance of selective reflection is about 10^{17}. In the recent work of Siekmann (8), and Cojan and Lennuier (2–6), selective reflection of the individual hyperfine structure components of Hg 2537Å was studied; the presence of selective reflection was evident at much lower vapor pressures because of the higher resolution of their methods of detection.

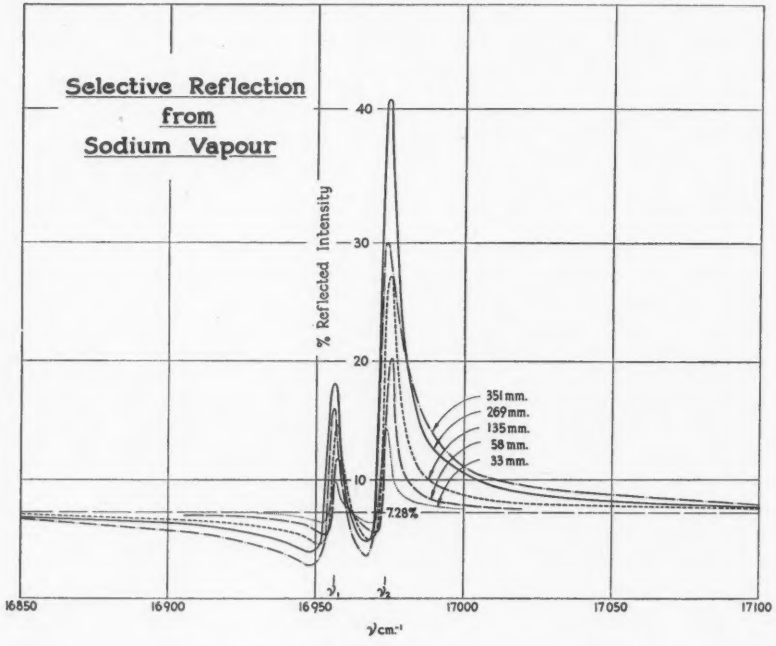

FIG. 2

Quantitative measurements of the selective reflection of sodium, potassium, and rubidium were obtained at pressures up to almost 1 atm. A set of intensity calibration curves for different frequencies covering the region of the selective reflection was used to reduce the photographic densities to intensities. Relative reflected intensities throughout the contour were obtained by taking the ratio of the intensities measured at the higher vapor pressures to those measured at low vapor pressure for which the reflection anomaly had a small extent. Finally "% reflected intensity" was obtained by assuming that the reflecting power outside of the region of anomalous reflection was equal to that calculated for a magnesium oxide-vacuum interface from the Fresnel reflection formula. For light at perpendicular incidence the calculated "normal reflected intensity" is 7.28% at the sodium resonance lines and 7.13% at the potassium and rubidium resonance lines, using the refractive indices of magnesium oxide given by Strong and Brice (9). This procedure was very satisfactory for reduction of the sodium data. For potassium and rubidium, however, owing to variations in emulsion sensitivity with wave length there was a possible error of about 5% in selecting the value of the relative intensity that should be put equal to the normal reflected intensity. This error has little effect on the deductions that are made from the experimental results. No quantitative results were obtained for caesium because of extreme variations in the sensitivity of Eastman 1-M plates which were used to photograph the caesium selective reflection.

A selection of experimental contours obtained for reflection from sodium vapor at pressures from 33 mm. to 351 mm. is shown in Fig. 2. The size of the reflection anomaly increases with increasing pressure except at the highest pressure where the intensity at the peaks has begun to decrease. A similar decrease in peak intensity was also observed for the higher pressures of potassium and rubidium. The falling-off of the peak intensity at high pressures was first observed for cadmium (10).

Interpretation of the Results

For light at normal incidence the reflecting power of a surface is given by the Fresnel formula:

$$R = \frac{(n - n')^2 + k^2}{(n + n')^2 + k^2},$$

where n and k are the refractive index and absorption coefficient of the reflecting medium, and n' is the refractive index of the bounding medium. For mercury and cadmium it was possible to calculate n and k for frequencies close to the resonance line using the dispersion equations written in terms of this single resonance frequency. However, for the alkali metals, the separation of the resonance doublet is so small that two-term dispersion equations must be used. These can be written:

$$n^2 - k^2 = n_0^2 + \frac{f_1 e^2 N}{2\pi m \nu_0}\left\{\frac{(\nu_1 - \nu)}{(\nu_1 - \nu)^2 + (\gamma_1/4\pi)^2} + \frac{2(\nu_2 - \nu)}{(\nu_2 - \nu)^2 + (\gamma_2/4\pi)^2}\right\}$$

$$2nk = \frac{f_1 e^2 N}{2\pi m \nu_0}\left\{\frac{\gamma_1/4\pi}{(\nu_1-\nu)^2+(\gamma_1/4\pi)^2}+\frac{2\gamma_2/4\pi}{(\nu_2-\nu)^2+(\gamma_2/4\pi)^2}\right\},$$

where n_0 ($\simeq 1$) is the hypothetical refractive index if no anomalous dispersion were present, ν_0 the mean of the resonance frequencies ν_1 and ν_2, N the number of atoms per cubic centimeter, γ the damping constant, f_1 the oscillator strength of the weaker line, and the other constants have their usual mean-

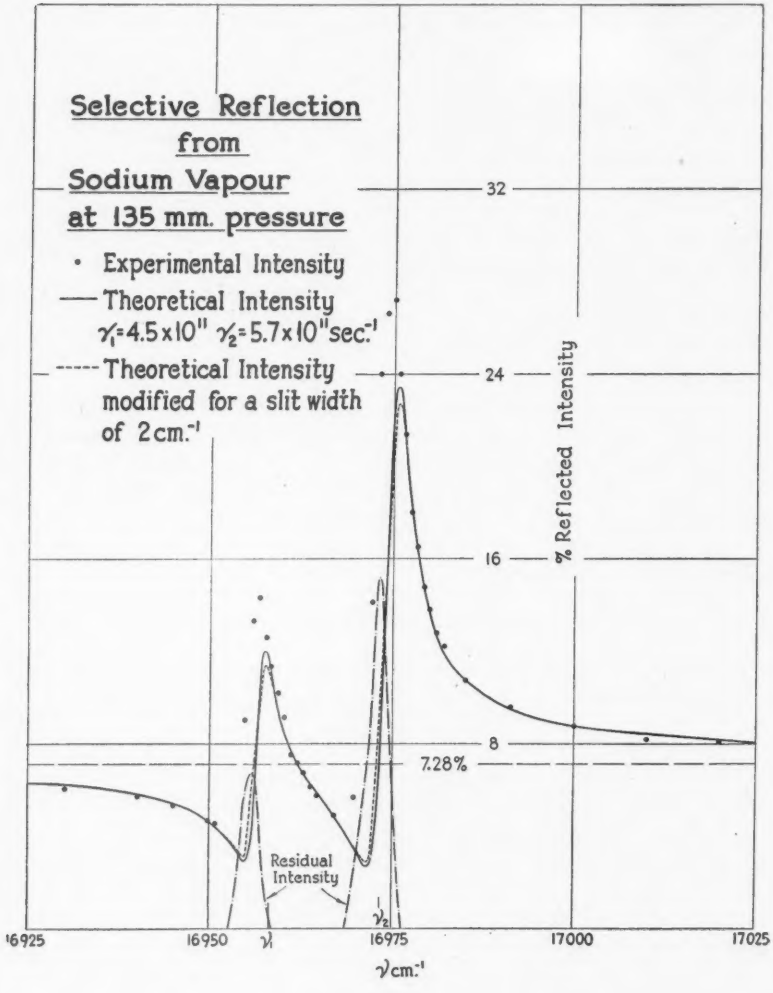

FIG. 3

ings. The oscillator strength of the stronger line, f_2, is equal to $2f_1$ as is well established for the alkali doublets.

In the wings of the contour γ and, consequently, k are negligible, and the oscillator strength can be calculated from the reflected intensity if N is known. This was the procedure used for mercury and cadmium. However, for the alkali metals, preliminary calculations showed that values of N obtained from the vapor pressure equations were not correct owing to inaccuracy in the temperature measurements. It was therefore necessary to use the known values

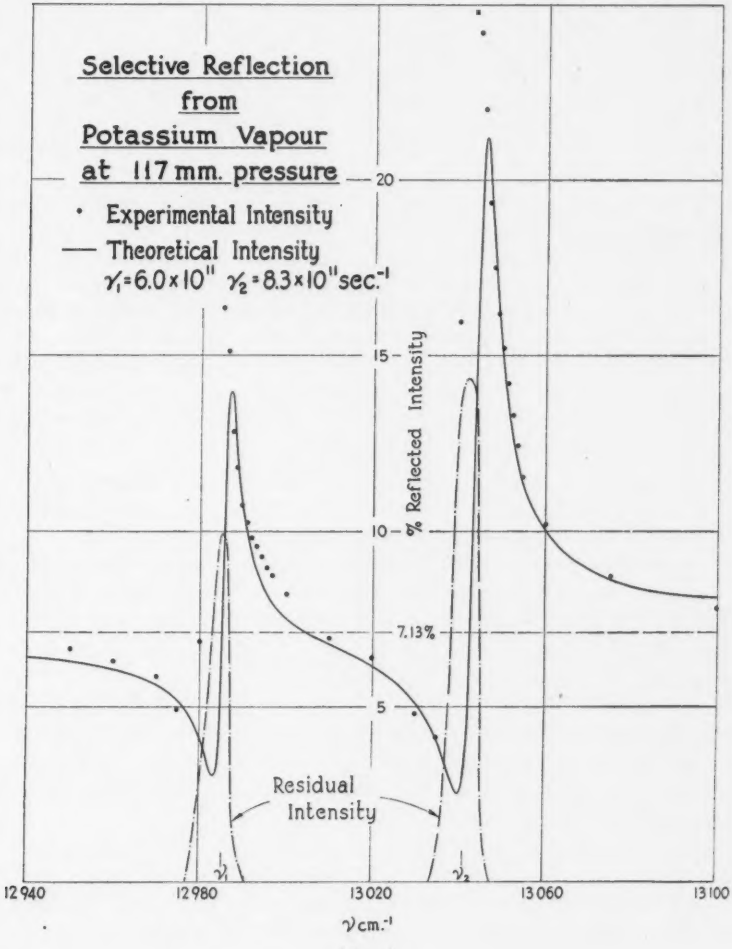

FIG. 4

of the oscillator strengths to calculate N from the reflected intensity in the wings of the pattern. The summary of Mitchell and Zemansky (7) shows that f_1 is very close to 0.33 for all the alkali metals.

To find theoretical curves to fit the experimental contours, values of γ_1 and γ_2 were selected and the dispersion equations solved for n and k at a series of frequencies by the method used previously (10). The reflection contour was then calculated using these values of n and k in the Fresnel formula. The difference between the calculated curve and the experimental contour indicated the adjustment required in γ. This trial and error process was repeated until theoretical curves in good over-all agreement with the experimental contours were obtained.

An example of the fitting is shown for sodium at 135 mm. pressure in Fig. 3 and for potassium at 117 mm. pressure in Fig. 4. At pressures above 1/2 atm. it was not possible, by adjusting γ, to obtain good agreement between theory and experiment. This departure of the experimental curve from the form predicted theoretically was also observed for cadmium at pressures above 5 atm. For all the alkali metals, when the theoretical contour giving the best over-all fit was subtracted from the experimental contour, lines of residual intensity were left about the resonance frequencies (Figs. 3 and 4). The residual intensity increases with increasing pressure; however, accurate quantitative conclusions concerning its variation with pressure and its relative magnitude for the two members of the doublet could not be drawn. The breadth of the residual line for the alkali metals is about 5 cm.$^{-1}$, for cadmium at low pressures about 12 cm.$^{-1}$; for mercury there was only a slight indication of its existence. The breadth of the residual intensity seems therefore to depend on the oscillator strength of the line.

Over a limited range of pressures it was possible to select values of γ to give a good over-all fit. The results are summarized in Table I. Column 2 gives the values of N calculated from the reflecting power in the wings of the contour. The values of the ratio, $\gamma/\sqrt{N}$, in columns 5 and 6, are seen to be reasonably constant for each line. This is in agreement with the empirical law, $\gamma \propto \sqrt{N}$, which was found to hold for mercury and cadmium.

Other regularities in the values of the damping constant are apparent from the table. For sodium and potassium the ratio γ_1/γ_2 is close to $1/\sqrt{2}$. This indicates that γ varies as $\sqrt{f}$ for the two lines of the doublet. Thus for each of these metals $\gamma/\sqrt{Nf}$, as given in columns 7 and 8 of the table, is practically the same for the two resonance lines. For rubidium the agreement is not so close; this is probably caused by a systematic error in the evaluation of the per cent reflected intensities.

The variation of $\gamma/\sqrt{Nf}$ from metal to metal suggests that γ may depend in a simple way on the frequencies of the resonance lines. The values of $\gamma\nu_0/\sqrt{Nf}$, averaged for the two resonance lines, are proportional to 1.10, 1.18, and 1.04 for sodium, potassium, and rubidium respectively. There is thus some evidence that γ varies as $\sqrt{Nf}/\nu_0$ for similar spectral transitions. For Hg 2537Å $\gamma\nu_0/\sqrt{Nf}$

is equal to 0.99, in good agreement with the alkali metals; however, for Cd 2288Å it is equal to 3.26, three times as great as for the other cases. The frequency dependence of γ therefore does not appear to be valid for all spectral transitions.

TABLE I

DAMPING CONSTANTS FOR SELECTIVE REFLECTION FROM THE ALKALI METAL VAPORS

	N atoms/cc. $\times 10^{-18}$	γ_1 sec.$^{-1}$ $\times 10^{-11}$	γ_2 sec.$^{-1}$ $\times 10^{-11}$	$\frac{\gamma_1}{\sqrt{N}}$ $\times 10^{-2}$	$\frac{\gamma_2}{\sqrt{N}}$ $\times 10^{-2}$	$\frac{\gamma_1}{\sqrt{Nf_1}}$ $\times 10^{-2}$	$\frac{\gamma_2}{\sqrt{Nf_2}}$ $\times 10^{-2}$
Na	0.34	2.3	3.0	4.0	5.2		
$\lambda_1$5896	0.57	3.0	3.8	4.0	5.0		
$\lambda_2$5890	0.93	3.8	4.9	4.0	5.1		
	1.25	4.5	5.7	4.0	5.1		
	2.4	6.0	7.9	3.9	5.1		
	3.1	6.8	–	3.7	–		
				Av. 3.9	5.1	6.8	6.2
K	0.86	4.9	6.8	5.3	7.3		
$\lambda_1$7699	1.31	6.0	8.3	5.2	7.2		
$\lambda_2$7665	2.1	7.6	10.2	5.3	7.1		
	3.5	9.8	13.5	5.2	7.2		
	4.2	10.9	–	5.4	–		
				Av. 5.3	7.2	9.2	8.9
Rb	0.55	3.8	4.5	5.1	6.1		
$\lambda_1$7948	0.84	4.9	5.7	5.3	6.2		
$\lambda_2$7800	1.34	6.4	6.8	5.5	5.9		
	1.8	6.8	9.4	5.1	7.0		
				Av. 5.3	6.3	9.2	7.3

The outstanding features of selective reflection as shown by the investigations on mercury, cadmium, and the alkali metals may be summarized as follows:

(*a*) Over a range of vapor densities, which varies for the different metals, the contour of the selective reflection can be explained in terms of the classical theory of reflection from an absorbing medium. The oscillator strength is independent of density and has a value which agrees with that found by other methods. The damping constant is proportional to $\sqrt{Nf}$ and thus differs fundamentally from the damping constant for collision broadening in emission and absorption which is proportional to Nf. This characteristic variation of the damping constant with the square root of the density may be due to the fact that selective reflection is a surface phenomenon.

(*b*) In most cases a residual intensity is left at the resonance frequency when the theoretical contour is subtracted from the experimental contour. This line probably has a close relationship to resonance fluorescence, and may be due to a second kind of selective reflection which has its origin in a coupling of the atoms absorbing and re-emitting resonance radiation at higher densities.

(*c*) At the higher vapor densities investigated the peak intensity of the selective reflection decreases and the pattern broadens more rapidly with in-

creasing density. This effect, which is not explicable in terms of the simple anomalous dispersion equations, might be understandable on the basis of a dispersion theory of coupled oscillators. It would be interesting to extend the experimental work to very high densities of a vapor with a strong resonance absorption. This might be possible using the resonance line of mercury at 1850Å, for which, however, selective reflection has not as yet been observed.

References

1. BRICE, R. T. Rev. Sci. Instruments, 8: 209. 1937.
2. COJAN, J. L. J. phys. radium, 9: 17S. 1948.
3. COJAN, J. L. and LENNUIER, R. Compt. rend. 228: 1409. 1949.
4. COJAN, J. L. and LENNUIER, R. Compt. rend. 228: 1710. 1949.
5. COJAN, J. L. Compt. rend. 231: 337. 1950.
6. LENNUIER, R. Compt. rend. 226: 708. 1948.
7. MITCHELL, A. and ZEMANSKY, M. Resonance radiation and excited atoms. Cambridge: The University Press, 1934. p. 146.
8. SIEKMANN, G. Ph.D. Dissertation, Berlin, 1940.
9. STRONG, J. and BRICE, R. T. J. Optical Soc. Am. 25: 207. 1935.
10. WELSH, H. L., KASTNER, J., and LAURISTON, A. C. Can. J. Research, A, 28: 93. 1950.
11. WOOD, R. W. Researches in physical optics. Vol. 2. Columbia Univ. Press. 1919.

THE SUDDEN INCREASE IN COSMIC RAY INTENSITY, NOVEMBER 19, 1949[1]

By D. C. Rose

Abstract

Cosmic ray counter telescopes were in continuous operation on November 19, 1949, at Ottawa (geomagnetic lat. 56.8°N) and at Resolute (geomagnetic lat. 83°N) in the Canadian Arctic. The two sets of apparatus were identical and consisted mainly of two counter telescopes, one with six inches and the other with 14½ inches of lead between counters. At Ottawa the counting rates of the individual counter trays were recorded as well as that of the coincidences.

On November 19 at about 1048 GMT a sudden increase occurred at Ottawa. The maximum intensity reached about 70% above normal in a few minutes, then decayed slowly to normal in about four hours. The increase was similar in both counter telescopes and in the individual counter trays. At Resolute an increase was noted but of a different type. The intensity did not rise suddenly but increased slowly to about 20% above normal and returned to normal again in about three hours, centered about 1140 GMT. These results and those of other observers indicate that the beam of rays responsible for this increase must strike the earth on a limited area only. Some deductions can be made about the extent of this area.

I. Introduction

On at least four occasions during more than a decade of continuous observation, cosmic ray records (7) have shown a phenomenal increase in intensity associated with solar flares. As recent calculations (2, 6, 8, 9) indicate that a solar source of cosmic rays, or at least a source within the local galaxy, may be acceptable, these solar flare effects are extremely important and should be studied in as much detail as possible.

Forbush, Stinchcomb, and Schein (7) published the results of the four cases which were observed with Compton–Bennett meters. The latest of these four, November 19, 1949, was the most intense noted up to the present, and other groups in France, Holland, and England (5, 4, 1) have published results of measurements taken at the same time.

The results* to be described in detail here were taken at Ottawa, Canada (geomagnetic lat. 56.8°N) and at Resolute (lat. 74°41′N, long. 94°55′W, geomagnetic lat. 83°N) in the Canadian Arctic. The station at Ottawa had been operating almost continuously since October 1, 1948. At Resolute the equipment was installed during August 1949 at the joint Canadian–American weather station. It was installed in a building used for ionosphere measurements operated by the Department of Transport of the Government of Canada. Except for a few minor equipment and power failures it has been in continuous operation since September 1, 1949.

II. Description of Apparatus

In planning the equipment for the two stations it was desirable that the two sets be identical. Power and space at Resolute were limited and fully automatic

[1] *Manuscript received November 11, 1950.*
Contribution from the Division of Physics, National Research Laboratories, Ottawa, Canada. Issued as N.R.C. No. 2364.
**NOTE: A short note on these results has already been published. (See ref. (10).)*

operation was essential. The experiment was planned therefore to get a maximum amount of information from four counter trays, two sets of double coincidence equipment, and a quadruple coincidence channel for measurements of showers. The arrangement of counter trays is shown in Fig. 1, which is approximately to scale. Each of the trays 1, 2, and 3 contains two brass counter tubes 1 in. in diameter and 16 in. effective length. Tray 4 contained five similar counters. The trays were made of 16 gauge aluminum. The whole apparatus was placed in a temperature controlled box. The total roof covering at Resolute consisted of about 2.5 in. of wood and some cork and glass wool insulation. At Ottawa the covering was rather less, consisting of about $1\frac{1}{4}$ in. of wood with 3 in. of rock wool insulation. Only light shielding (1 in. of lead) was placed under the bottom tray as the apparatus was either at floor level close to ground or just over a thick concrete roof.

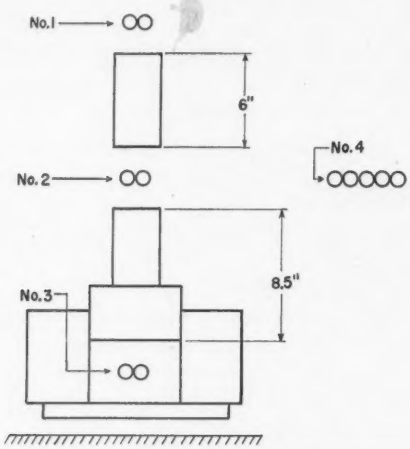

FIG. 1. *Arrangement of counter trays and lead absorber.*

The lead shielding between counters was arranged so that by using two coincidence channels the intensity could be measured simultaneously through two different thicknesses. Coincidences between trays 1 and 2 represent the vertical intensity through 6 in. of lead, and between 1 and 3, the vertical intensity through $14\frac{1}{2}$ in. of lead. The counts in tray 3 were recorded separately, giving nondirectional intensity, with a minimum shielding of 4 in. of lead on the sides and a greater amount on top. Coincidences were also recorded between trays 2 and 4, as the (1, 3) channel combined with the (2, 4) was used to record quadruple coincidences. The (2, 4) results are of little interest, largely representing soft horizontal particles, and the quadruples, representing showers with penetrating particles, came at too low a rate to show any significant increases at the time of the solar flare. Therefore, they will not be considered further in this paper. At Ottawa the counts of each individual tray and the coincidence

channels were recorded, but at Resolute the records were limited to tray 3 and the coincidence channels.

The electronic components of the equipment will be described in a separate publication and will be discussed only briefly here. In each tray there was a partial quenching circuit designed to increase the life of the counter tubes (alcohol and argon filled) and to reduce the tendency to double counts. This was followed by a cathode follower stage to reduce the impedance so that long cables could be used. Pulse shaping and discriminator circuits followed, and coincidences were formed by adding the pulse at the grid of a pentode rather than by the more conventional Rossi circuit. The time resolution was about two microseconds. A cross checking system was used wherein the coincidence mixing circuits are duplicated, and by watching duplicate outputs on scalers the behavior of the whole system can be checked accurately. Continuous checking was carried out at Ottawa, and periodic spot checks at Resolute. The scalers were binary types with four and eight stages. At Ottawa some early models with three stages were used on the coincidence channels. Every time a scaler completed its cycle this was indicated on a message register and also was recorded on the paper tape of an Esterline Angus 20-pen operation recorder. Time marks were also put on the Esterline Angus tape every minute. The tape moved at the rate of a foot an hour so that the time of each cycle of the scalers could be observed to within a few seconds.

This system of recording gives a great deal of detail. Averages over a long period (12 and 24 hr.) were usually recorded by reading the message registers. For more detail the "pips" on the tape of the 20-pen recorder were counted. Hence any period of averaging could be used down to the time involved in the completion of one cycle of the scalers. Ordinarily, for studying meteorological variations in intensity four-hour averages were taken, but, at the time of the solar flare effect, periods down to two to three minutes were used.

III. Results

Fig. 2 shows a plot of the variation in intensity at Ottawa on November 19 to 21. The abscissa represents GMT and the ordinate, the percentage of the mean taken for about 18 hr. before the solar flare effect. Fig. 3 shows the same results for Resolute. The points plotted before 0800 GMT on November 19 are four-hour averages in the case of Fig. 2 and one-hour averages in the case of Fig. 3. In both figures the points shown on the days following November 19 are four-hour averages. The period of averaging was shortened immediately before and during the increase in intensity. To get detail here, the time interval between one to five pips (depending on the channel concerned) was measured; therefore, the plotted points indicate an average over varying periods of two to three minutes. At the height of the peak these intervals were overlapped to give a maximum of detail without too high a statistical error. In Figs. 2 and 3 the time scale between 1030 and 1330 hours has been expanded as shown. The accuracy is indicated by vertical bars representing twice the square root of the

number of counts during the period of averaging expressed as a percentage of the counting rate at the time where the bar appears. These accuracies are shown with each curve, for the four-hour period (except in the case of counter trays 1, 4, and 3, wherein the statistical error is about equal to the thickness of the dots) and for the shortest period used at the height of the peak. All

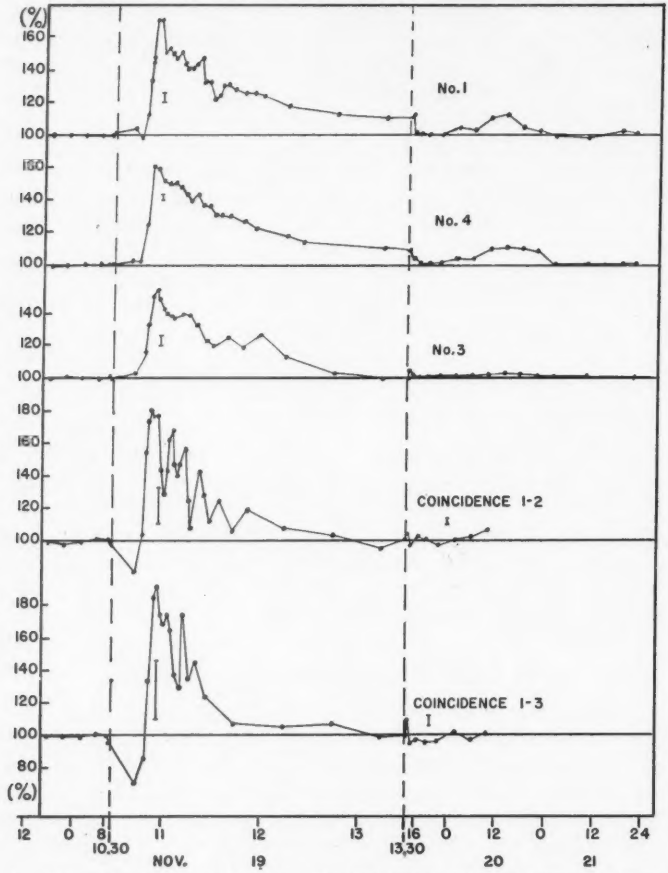

FIG. 2. *The sudden increase at Ottawa. The time scale is expanded between 10.30 and 13.30 GMT on November 19.*

other points will have an accuracy somewhere between these extremes. Since the increase was not as sudden at Resolute as at Ottawa the shortest period used for averaging was 20 min.

Table I shows the mean counting rates for each recorded channel before the solar flare, the maximum height of the increase, and the error represented by

the square root of the number of counts during the shortest time interval. The statistical error in the magnitude of the increase, if it were separated from the background, would be somewhat higher than is indicated by the percentage errors in Table I and the bars in Figs. 2 and 3. The errors as shown however serve in estimating the significance of changes in intensity where such significance may be questionable. The actual height of the peak at Ottawa is difficult to estimate accurately, as the maximum intensity lasted for such a short period.

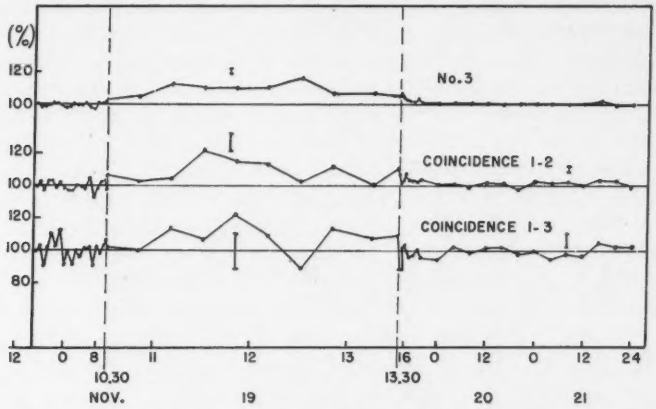

FIG. 3. *The increase at Resolute. The time scale is expanded between 10.30 and 13.30 GMT.*

TABLE I

Counter tray or coincidence channel	Rate per min. before increase	Height of peak in % of mean	Error at top of peak in %
Ottawa			
1	348	170	2.8
4	816	162	1.5
3	199	155	2.8
(1, 2)	16.4	180	11.0
(1, 3)	4.5	192	18.0
Resolute			
(1, 2)	16.5	122	5.5
(1, 3)	4.5	122	10.0
3	197	112	1.5

IV. Discussion

The difference between the increases at Ottawa and at Resolute is very striking. The Ottawa record shows the typical solar flare increase—a very sudden rise in intensity followed by a decay resembling an exponential curve.

The increase at Resolute started gradually, the intensity remaining high for over an hour then it returned to normal slowly as is shown in Fig. 3. It is centered on the time scale at about 1140 GMT—definitely later than the increase noted at other North American stations, but more consistent in time with the increase noted by Dauvillier (5).

As the Resolute increase is small its significance was examined carefully in view of meteorological and statistical variations. In the case of tray 3 and the (1, 2) coincidence channel the intensity change was enough above expected statistical variations to indicate a very high probability that it is real. The counting rate in the (1, 3) coincidence channel is so low that the increase in this case is not clearly shown. At the time it occurred there were no meteorological conditions that would account for such a short-period increase of the magnitude found. The four-hour averages were plotted for a period of several months to see whether such occurrences were common. Though individual counters near the end of their lives occasionally run fast for short periods, there were no other occasions where increases were noted simultaneously in independent recording channels and only one case where an unexplained increase occurred in one counter tray. It seems justifiable therefore to assume that the increase found at Resolute is real, though were it of much lower magnitude its significance would be questionable.

The Ottawa results show roughly the same percentage increase for lightly shielded counters, and for coincidence channels with up to $14\frac{1}{2}$ in. of lead. Table I shows differences in the maximum height of the peak but the intensity over the short period where it is a maximum is difficult to measure accurately. The decay rate seems to be appreciably different in the results from different recorded channels. The decay to normal intensity is slowest in the case of trays 1 and 4 and quickest in the case of the (1, 3) coincidence channel, which has the thickest absorber. If this is significant it could be the result of some directional effect in the rays causing the increase. The shape of the decay part of the peaks at Ottawa was examined carefully to see whether any secondary peak was apparent which might match the Resolute results. There is no evidence of matching between the two stations.

Besides the sudden increase and its decay, the curves in Fig. 2 show other variations in intensity. The results from the two coincidence channels show a decrease just before the sudden increase which is large enough to indicate a reasonable probability that it is real. Its significance however is not apparent. There is also a small increase (about 10%) lasting nearly a day (November 20–21) in the unshielded counter tray results (Nos. 1 and 2). This is almost certainly a meteorological variation. Meteorological changes in intensity of the soft component are known to be great, particularly when the measuring apparatus is sensitive to gamma rays from radioactive matter brought down by precipitation.

No corrections were made for barometric variations, as it is very doubtful whether such corrections would enhance the value of the results. Analyses of

intensity in relation to barometric pressure have been made for both stations, and barometer coefficients were calculated (11). The correlation coefficients are so low that no significance can be given to individual variations in intensity of a few per cent spread over many hours. No importance therefore is attached to indicated differences of a few per cent in the intensity levels for periods before and after the solar flare effect.

On two other occasions where a sudden increase was observed (7) it was followed some hours later by a sudden decrease of the order of 10% which took some days to recover. A third case of such a decrease was reported by Chakroborty and Chatterjee (3). These decreases coincide with the "sudden commencement" of a magnetic disturbance. On the November 19, 1949, occasion no sudden decrease of corresponding magnitude occurred at any of the stations that have reported results.

When the results of Forbush, Stinchcomb, and Schein (7), Dauvillier (5), and Clay and Jongen (4) are considered with the above measurements a rough picture may be deduced of areas where the beam causing increase in intensity struck the earth. Forbush *et al.* found increases of about 30% and 40% above background at Godhavn and Cheltenham respectively, a much greater increase at Climax (3500 m. above sea level), none at Huancayo and about 25% at Christchurch, New Zealand. Assuming that the great increase at Climax (180% above background) is due to altitude, their results alone suggest a normal latitude effect with an intense soft component causing the enhanced effect at high altitude. The small increases at Resolute and in European stations indicate however that the world-wide effect is more complicated. The intensity of the increase at Ottawa was significantly higher than that at Cheltenham and at Godhavn and therefore is not consistent with a normal latitude effect. An exact intensity comparison between counter measurements and ionization chamber measurements is of course, not too reliable, but, for the same spectrum and shielding, intensity variations measured by the two methods should not differ greatly.

Though the Ottawa results show small differences in the intensity increase measured under different absorber thicknesses the significance of these differences is hardly definite. The general similarity in the height and shape of the peaks suggests that the rays causing the increase are similar in nature and spectrum to normal cosmic rays. The phenomenal increase at Climax may therefore be due to its geographical position rather than its altitude. The intensities recorded at different stations can then be explained by assuming that the rays responsible for the increase strike the earth in a narrow cone, perhaps of irregular shape or perhaps sweeping across the surface of the earth like the path of a total solar eclipse.

If the latter is assumed, some information about its path can be deduced. As the highest recorded increase occurred at Climax the center of the path is assumed to pass through that point. The increase at Cheltenham is slightly greater than that at Godhavn. Therefore the path should pass between these

two, slightly nearer Cheltenham. This puts Ottawa nearer the center of the path than either Cheltenham or Godhavn and therefore is consistent with the magnitude of the increase noted here. The path would then move out over the Atlantic Ocean, missing Western Europe. Such a path is shown in Fig. 4 with the location of the stations where observations were taken.

The small effects at Resolute and Dauvillier's results both occurring at a time later than that of the increase at other stations could be imagined to be some shadow or penumbra effect possibly due to particles in a different orbit. This narrow cone cannot represent the whole picture, as the results at Christchurch

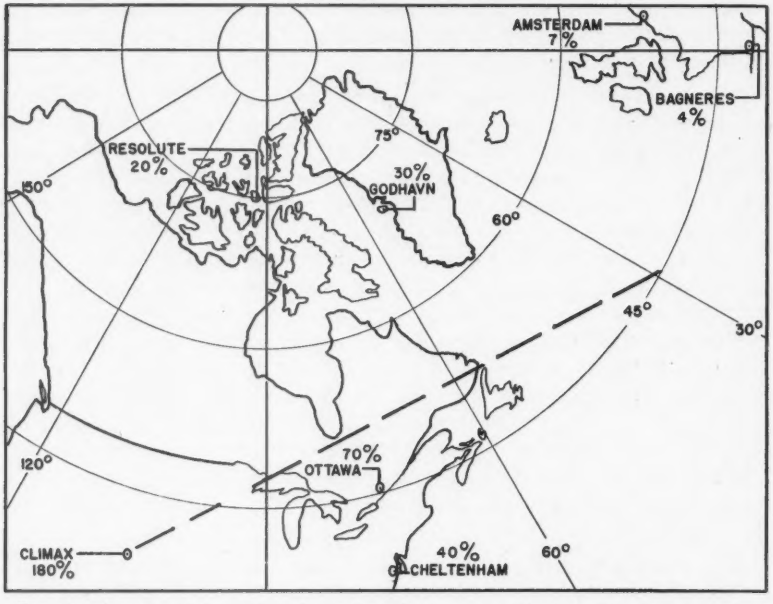

FIG. 4. *A section of the northern hemisphere showing a possible center line of a narrow beam that could produce the observed results.*

indicate that something is also happening in the southern hemisphere. The possibility of such a beam of particles striking the earth in equatorial regions on some occasion is indicated by the results of Chakroborty and Chatterjee (3) who found some evidence of an increase on January 25, 1949, even though they observed only the decay part of the increase. Their ionization chamber was not in operation when it started.

Such a narrow cone of particles must be only about 3000 miles wide on the surface of the earth. This would subtend a very small angle at the sun, particularly as the path would not be rectilinear. At 1045 GMT on November 19 the sun would not have risen over the North American continent.

V. Summary of Conclusions

The measurement of the sudden increase in intensity on November 19 at Ottawa indicates that the percentage increase is of the same order for lightly shielded counters and for double coincidence units with as much as $14\frac{1}{2}$ in. of lead between counters. The results show a slightly higher increase in the harder rays and some differences in the shape of the decay in intensity but the significance of these is questionable. It seems likely therefore that the increase is due to rays of the same nature as normal cosmic rays, at least in so far as their effect at sea level is concerned At Resolute in the Canadian Arctic the increase was relatively small, of a different form, and centered somewhat later in time.

These results, combined with other measurements by Forbush, Stinchcomb, and Schein, Dauvillier, and Clay and Jongen, suggest that the rays causing the main increase strike the earth in a narrow cone which in the northern hemisphere crosses the North American continent but does not strike Europe. Some weaker cone or penumbra effect in a different path may account for the smaller and more delayed effect at Resolute.

Acknowledgments

The measurements at Resolute were made possible through the co-operation of the Department of Transport of the Canadian Government. Both the Meteorological and Radio Divisions of that Department assisted. The apparatus was transported to Resolute by the United States Navy Supply Mission to the Joint Weather Stations in the Arctic. The services of Mr. John Galt are particularly appreciated for the operation of the equipment.

References

1. Adams, N. Phil. Mag. 41: 503. 1950.
2. Alfven, H. Phys. Rev. 75: 1732. 1949.
3. Chakraborty, I. L. and Chatterjee, S. D. Indian J. Phys. 23: 525. 1949.
4. Clay, O. and Jongen, H. F. Phys. Rev. 79: 908. 1950.
5. Dauvillier, A. Compte. rend. 229: 1096. 1949.
6. Forbush, S. E., Gill, P. S., and Vallarta, M. S. Revs. Modern Phys. 21: 44. 1949.
7. Forbush, S. E., Stinchcomb, T. B., and Schein, M. Phys. Rev. 79: 501. 1950.
8. Kane, E. O., Shanley, T. J. B., and Wheeler, J. A. Revs. Modern Phys. 21: 51. 1949.
9. Richtmyer, R. D. and Teller, E. Phys. Rev. 75: 1729. 1949.
10. Rose, D. C. Phys. Rev. 78: 181. 1950.
11. Rose, D. C. Can. J. Phys. 29: 97. 1951.

STATISTICS OF A LINEAR PARAMAGNETIC MACROMOLECULE[1]

By W. Opechowski and J. M. Bryan

Abstract

The partition function of a linear "macromolecule" composed of N paramagnetic atoms subject to the Ising interaction is calculated for an arbitrary N. From the partition function the expressions for the specific heat and the initial paramagnetic susceptibility are obtained. It is shown on the example of the susceptibility that the procedure, customary in statistical mechanics, which consists in using the asymptotic expressions ($N \to \infty$) to describe actual physical systems (N very large, but finite) should be used with some caution in the region of very low temperatures.

Introduction

We consider in this paper a finite linear chain of paramagnetic atoms which interact with one another in a way first discussed by Ising (2). In particular, we calculate the magnetic susceptibility of such an Ising "macromolecule". The problem in itself is not a very exciting one. Our fictitious macromolecule is not likely to constitute a suitable model for any actual macromolecule. However, the Ising interaction has been extensively used (see, for instance, Kramers and Wannier (4); Onsager (5); Kaufmann and Onsager (3)) to obtain some idea of what happens in the case of the exchange interaction, which is much more difficult to treat rigorously, and also in the case of the order–disorder transformations in binary alloys. Even in the case of the Ising interaction, a rigorous calculation of the partition function has so far been performed only for an infinite linear chain of atoms and for various types of infinite two-dimensional crystals.* Undoubtedly, the limiting case in which the number N of atoms composing the system tends to infinity is the most interesting one, because only in that case is there a possibility for sharply defined transition points to occur. Nevertheless, the fundamental question remains to what extent the equations derived for $N \to \infty$ represent a satisfactory description of actual physical systems, for which N is necessarily finite, however large it might be. It is just with this question in mind that we have carried out the calculations presented in this paper. We chose the Ising linear model because of its simplicity. There are probably not many other reasonable physical models for which a closed analytic formula for the partition function could be obtained for an arbitrary N.

Assumptions Regarding the Macromolecule

What we have called an Ising macromolecule is a linear chain of N equidistant identical atoms. Each atom carries a magnetic dipole μ which is capable of only two orientations. The interaction energy between two

[1] *Manuscript received December 18, 1950.*
Contribution from the Department of Physics, the University of British Columbia, Vancouver, B.C.

* *It should be mentioned, however, that some numerical calculations for small values of N and no magnetic field have been done by Fokker* (1).

adjacent atoms depends only on the relative orientation of their dipoles; the contribution of a given pair of adjacent atoms to the total energy of the macromolecule changes its sign but not its absolute value if the two corresponding dipoles change their relative orientation from a parallel to an antiparallel one or vice versa. There is no interaction between atoms which are not direct neighbors.

A state of the macromolecule is determined by specifying the orientation, with respect to some fixed direction, of all N dipoles. On the basis of these assumptions, the energy E of a given state is:

$$E = \tfrac{1}{2} JQ_{+-} - \tfrac{1}{2} J(Q - Q_{+-}) + \mu H(Q_- - Q_+) , \tag{1}$$

where

Q is the total number of pairs of adjacent atoms (i.e., $Q = N - 1$);

Q_{+-} is the number of pairs of adjacent atoms whose dipoles are antiparallel to each other;

$Q_+(Q_-)$ is the number of dipoles parallel (antiparallel) to the homogeneous magnetic field H;

J is a constant of interaction which plays here the same part as the exchange integral in the Heisenberg model of ferromagnetism; J may be positive or negative, these two cases corresponding to interactions of ferromagnetic or antiferromagnetic type respectively.

In order to put Equation (1) into a form suitable for calculation of the partition function, we first number all atoms of the macromolecule, beginning at one of its ends: 1, 2, 3, ... N. Second, we characterize each state of the macromolecule by a set of N numbers $\sigma_1, \sigma_2, \sigma_3 \ldots \sigma_N$, σ_k being -1 if the dipole of the k-th atom is antiparallel with respect to the direction of H, and $+1$ if the dipole is parallel. Expressing Q_{+-} in terms of the σ's we have:

$$Q_{+-} = \tfrac{1}{2} \sum_{k=1}^{N-1} (1 - \sigma_k \sigma_{k+1}). \tag{2}$$

Equation (1) may be then rewritten as

$$E = - \tfrac{1}{2} J \sum_{k=1}^{N-1} \sigma_k \sigma_{k+1} - \mu H \sum_{k=1}^{N} \sigma_k. \tag{3}$$

The partition function Z_N of the macromolecule is therefore:

$$Z_N = \sum_{\sigma_1=\pm 1} \cdots\cdots \sum_{\sigma_N=\pm 1} \exp\left\{\Theta \sum_{k=1}^{N-1} \sigma_k \sigma_{k+1} + \alpha \sum_{k=1}^{N} \sigma_k\right\}, \tag{4}$$

where

$$\Theta = \frac{J}{2kT}, \quad \alpha = \frac{\mu H}{kT}, \tag{5}$$

k and T being the Boltzmann constant and the absolute temperature respectively. Hence, the free energy F_N of the macromolecule is:

$$F_N = - kT \log Z_N. \tag{6}$$

We shall be interested, in particular, in the specific heat C_N and the initial paramagnetic susceptibility X_N of the macromolecule. These are obtained from the free energy by differentiation:

$$C_N = -T\left(\frac{\partial^2 F_N}{\partial T^2}\right)_{H=0}, \quad X_N = -\left(\frac{\partial^2 F_N}{\partial H^2}\right)_{H=0}. \tag{7}$$

Calculation of the Partition Function

One way of calculating Z_N begins with rewriting Equation (4) as

$$Z_N = Z_N^+ + Z_N^-, \tag{8}$$

where

$$Z_N^{\pm} = \sum_{\sigma_1} \cdots \sum_{\sigma_N} \exp\left\{\theta\left(\sum_{k=1}^{N-2} \sigma_k \sigma_{k+1} \pm \sigma_{N-1}\right) + \alpha\left(\sum_{k=1}^{N-1} \sigma_k \pm 1\right)\right\}. \tag{9}$$

Then the following pair of recurrence relations results immediately:

$$\left.\begin{aligned} Z_{N+1}^+ &= e^{\theta+\alpha} Z_N^+ + e^{-\theta+\alpha} Z_N^-, \\ Z_{N+1}^- &= e^{-\theta-\alpha} Z_N^+ + e^{\theta-\alpha} Z_N^-; \end{aligned}\right\} \tag{10}$$

$Z_{N+1}^{\pm}$ refer, of course, to a macromolecule composed of $N+1$ atoms which is obtained from that composed of N atoms by adding one extra atom at one of the ends. Although Equations (10) have so far been established for $N \geqq 2$ only, it is easy to verify that they will hold also for $N = 1$, provided we define Z_1 as the partition function of one free atom in the presence of the magnetic field:

$$Z_1 = e^{\alpha} + e^{-\alpha} \text{ and } Z_1^{\pm} = e^{\pm\alpha}. \tag{11}$$

The idea of splitting up the partition function into two terms, in the way indicated by Equations (8) and (10), in order to obtain the recurrence relations is due to Kramers and Wannier (4). However, Kramers and Wannier were interested in the case that N tends to infinity and for that reason wrote Equations (10) in a form already adjusted to this special case.*

Starting from Equations (10) it is easy to show that the partition function is given, for any $N \geqq 1$, by the matrix equation:

$$Z_N = \left(e^{\frac{\alpha}{2}}, e^{-\frac{\alpha}{2}}\right)\begin{pmatrix} e^{\theta+\alpha}, & e^{-\theta} \\ e^{-\theta}, & e^{\theta-\alpha} \end{pmatrix}^{N-1}\begin{pmatrix} e^{\frac{\alpha}{2}} \\ e^{-\frac{\alpha}{2}} \end{pmatrix}. \tag{12}$$

The problem is thus reduced to calculating arbitrary powers of the matrix

$$\begin{pmatrix} e^{\theta+\alpha}, & e^{-\theta} \\ e^{-\theta}, & e^{\theta-\alpha} \end{pmatrix}, \tag{13}$$

which is easily done using a procedure suggested by Montroll and quoted by Kramers and Wannier (4). Although we have carried out these calculations,

* *Kramers and Wannier did calculate, for any value of N, the partition function of a closed ring of N atoms. We shall later quote and use their result.*

we prefer to follow here another, more straightforward way of obtaining the same results.

This other way of calculating Z_N starts from the single recurrence relation

$$Z_{N+2} = e^{\Theta}(e^{\alpha} + e^{-\alpha}) Z_{N+1} - (e^{2\Theta} - e^{-2\Theta}) Z_N, \tag{14}$$

whose validity may be checked directly, or proved by adding the two Equations (10) side by side and using Equation (8).

First, we show that

$$Z_{N+1} = a(\lambda_1^{N+1} + \lambda_2^{N+1}) + b(\lambda_1^N + \lambda_2^N), \tag{15}$$

where a and b are arbitrary constants, is a solution of Equation (14), provided

$$\lambda_1 + \lambda_2 = e^{\Theta}(e^{\alpha} + e^{-\alpha}), \quad \lambda_1 \lambda_2 = e^{2\Theta} - e^{-2\Theta}, \tag{16}$$

or

$$\lambda_1 = e^{\Theta}[\cosh \alpha + (\sinh^2 \alpha + e^{-4\Theta})^{\frac{1}{2}}], \quad \lambda_2 = e^{\Theta}[\cosh \alpha - (\sinh^2 \alpha + e^{-4\Theta})^{\frac{1}{2}}]. \tag{17}$$

Multiplying both sides of Equation (15) by $\lambda_1 + \lambda_2$, we find after making use of that equation again:

$$(\lambda_1 + \lambda_2) Z_{N+1} = Z_{N+2} + \lambda_1 \lambda_2 Z_N. \tag{18}$$

This is identical with Equation (14), if Equations (15) are satisfied.

We may note in passing that the Recurrence Relation (14) may be obtained, upon using Equation (12), directly from the previous matrix formulation by observing that the Matrix (13) must satisfy its own characteristic equation, whose roots are just λ_1 and λ_2. This establishes the link between the two methods of calculating Z_N.

Next, we determine the two constants a and b. Equation (15) has the form of an inhomogeneous linear equation in a and b, so that we shall be able to find a and b as soon as we know the term on its left-hand side for two different values of N. Now, the very simple calculation that leads from (15) to (18) is obviously valid even for $N = 0$, so that we may determine a and b from the two equations obtained by putting in (15) $N = 0$ and $N = 1$:

$$\begin{aligned} Z_1 &= a(\lambda_1 + \lambda_2) + 2b \\ Z_2 &= a(\lambda_1^2 + \lambda_2^2) + b(\lambda_1 + \lambda_2). \end{aligned} \tag{19}$$

Solving Equations (19) with respect to a and b, we find:

$$\begin{aligned} a &= \frac{2Z_2 - (\lambda_1 + \lambda_2)Z_1}{(\lambda_1 - \lambda_2)^2}, \\ b &= \frac{[(\lambda_1 + \lambda_2)^2 - 2\lambda_1 \lambda_2] Z_1 - (\lambda_1 + \lambda_2)Z_2}{(\lambda_1 - \lambda_2)^2}. \end{aligned} \tag{20}$$

These equations when combined with Equation (15) yield

$$Z_N = C_1 \lambda_1^{N-1} + C_2 \lambda_2^{N-1}, \tag{21}$$

where $$C_1 = \frac{\lambda_2 Z_1 - Z_2}{\lambda_2 - \lambda_1}, \quad C_2 = \frac{\lambda_1 Z_1 - Z_2}{\lambda_1 - \lambda_2}. \tag{22}$$

Now, Z_1 is given by (11); we calculate Z_2 directly from (4):

$$Z_2 = e^{\Theta}(e^{2\alpha} + e^{-2\alpha}) + 2e^{-\Theta}. \tag{23}$$

Finally, using Equations (21), (22), (11), (23), and (17) we obtain:

$$Z_N = \left(\cosh\alpha + \frac{\sinh^2\alpha + e^{-2\Theta}}{\sqrt{\sinh^2\alpha + e^{-4\Theta}}}\right)[e^{\Theta}(\cosh\alpha + \sqrt{\sinh^2\alpha + e^{-4\Theta}})]^{N-1}$$

$$+ \left(\cosh\alpha - \frac{\sinh^2\alpha + e^{-2\Theta}}{\sqrt{\sinh^2\alpha + e^{-4\Theta}}}\right)[e^{\Theta}(\cosh\alpha - \sqrt{\sinh^2\alpha + e^{-4\Theta}})]^{N-1}. \tag{24}$$

The expression for the free energy F_N of the macromolecule follows immediately by substituting (24) into (6).

For $N \to \infty$, the free energy per atom $f_N = F_N/N$ reduces, as can be seen from Equations (24) and (6), to the well known expression:

$$f_\infty = -kT \log \lambda_1. \tag{25}$$

Equation (25) could have been obtained directly from the Recurrence Relation (14). In fact, for $N \to \infty$, the ratio Z_{N+1}/Z_N must become independent of N, so that

$$\frac{Z_{N+2}}{Z_N} \approx \left(\frac{Z_{N+1}}{Z_N}\right)^2 \qquad (N \to \infty).$$

Hence, Equation (14) goes over into a quadratic equation in Z_{N+1}/Z_N whose larger root is λ_1. This means that, for $N \to \infty$,

$$Z_N \approx q\lambda_1^N \quad (N \to \infty),$$

where q does not depend on N, so that with the aid of (6), Equation (25) follows immediately.

Specific Heat and Magnetic Susceptibility

Making use of Equations (6), (7), and (24), we obtain, after some elementary calculations, the following expressions for the atomic heat $c_N = C_N/N$ and the atomic magnetic susceptibility $\chi_N = X_N/N$ of a macromolecule composed of N atoms:

$$\frac{c_N}{k} = \left(1 - \frac{1}{N}\right)\left(\frac{\Theta}{\cosh\Theta}\right)^2, \tag{26}$$

$$\frac{J}{2\mu^2}\chi_N = \Theta e^{2\Theta}\left[1 - \frac{\sinh 2\Theta}{N}(1 - \tanh^N\Theta)\right], \tag{27}$$

where, as previously,

$$\Theta = \frac{J}{2kT},$$

J being positive or negative ("ferromagnetic" or "antiferromagnetic" case).

For $N \to \infty$ and a fixed value of Θ, these equations reduce to

$$\frac{c_\infty}{k} = \left(\frac{\Theta}{\cosh \Theta}\right)^2, \tag{28}$$

$$\frac{J}{2\mu^2}\chi_\infty = \Theta e^{2\Theta} \qquad \left(\text{i.e., } \chi_\infty = \frac{\mu^2}{kT}\, e^{\frac{J}{kT}}\right). \tag{29}$$

Equations (28) and (29) have already been derived by others (see, for instance, Kramers and Wannier (4)), and can, of course, very easily be obtained directly from Equation (25).

The difference between the expression for c_∞ and that for c_N is rather trivial: c_∞ obviously does represent a good approximation to c_N for any T if N is sufficiently large.

The situation is less simple in regard to χ_∞ and χ_N.

If the temperature is not too low ($|\Theta|$ not too large), Equation (29) obviously may be used as a satisfactory approximation formula also for finite N, provided N is sufficiently large. In fact, the ratio χ_N/χ_∞ tends to unity for any N as the temperature increases indefinitely ($\Theta \to 0$), and the macromolecule behaves like an assembly of N free atoms, each obeying the same Curie law:

$$\chi_N \approx \chi_\infty = \frac{\mu^2}{kT} \quad (T \to \infty). \tag{30}$$

In the region of low temperatures ($|\Theta|$ large), it may happen, however, that Equation (29) does not represent a correct approximation to the actual temperature dependence of the susceptibility of the macromolecule, even if N is very large. In fact, for any fixed value of N, however large it might be, there always exists a temperature below which the temperature dependence of χ_∞ widely differs from the temperature dependence of χ_N. Mathematically speaking, the convergence of $\chi_N(T)$ to $\chi_\infty(T)$ is not uniform. It follows that χ_∞ can no longer be used as an approximate formula for the susceptibility of a macromolecule, which is necessarily composed of a finite, fixed number of atoms.

The truth of these statements may be seen from the form that Equation (27) assumes when the temperature tends to zero ($|\Theta| \to \infty$), N being kept constant: in the region of temperatures for which the condition

$$kT/|J| \ll 1/\log 2N \tag{31}$$

is satisfied Equation (27) reduces either to

$$\chi_N \approx \frac{1}{N}\frac{(N\mu)^2}{kT} \qquad (T \to 0,\ J > 0) \tag{32}$$

or to

$$\chi_N \approx \frac{1}{N}\frac{\mu^2}{kT}\left\{\tfrac{1}{2}[1-(-1)^N] + Ne^{\frac{J}{kT}}[1+(-1)^N]\right\} \qquad (T \to 0,\ J < 0). \quad (33)$$

The physical interpretation of these equations is very simple. At sufficiently low temperatures, the lowest energy state of the macromolecule plays the decisive part, at least if the lowest state is magnetic at all.

If J is positive, the lowest state corresponds to all dipoles being lined up, so that the macromolecule behaves like a free dipole of magnitude $N\mu$. Consequently, we obtain for the susceptibility the Curie law expressed by Equation (32).

If J is negative and N is odd, all dipoles but one are "paired" in the lowest state, so that the macromolecule behaves like a free dipole of magnitude μ, which leads again to the Curie law with a correspondingly smaller value of the Curie constant:

$$\chi_N \approx \frac{1}{N}\frac{\mu^2}{kT} \qquad (T \to 0,\ J < 0,\ N \text{ odd}). \quad (34)$$

If J is positive and N is even, all dipoles are "paired" in the lowest state, so that this state is not magnetic and gives no contribution at all to the susceptibility. Consequently, the part played by the lowest state in the two previous cases is taken over by the first "excited" state (which is highly degenerate). Hence, the exponential decrease of the susceptibility with the decreasing temperature:

$$\chi_N \approx \frac{1}{N}\frac{2\mu^2}{kT}\,Ne^{-\frac{|J|}{kT}} \qquad (T \to 0,\ J < 0,\ N \text{ even}). \quad (35)$$

To get an estimate of the order of magnitude of the temperature below which Equation (29) is certainly not valid, we evaluate Inequality (31) numerically.

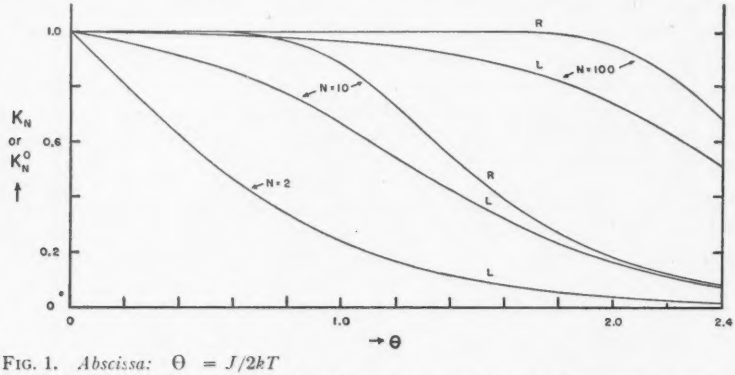

FIG. 1. *Abscissa:* $\Theta = J/2kT$
Ordinate: $K_N = \chi_N/\chi_\infty$, *for linear macromolecules; the corresponding curves are marked with L.*
$K_N^0 = \chi_N^0/\chi_\infty$, *for ring macromolecules; the corresponding curves are marked with R.*

In so far as the Ising interaction between atoms of a linear macromolecule can be ascribed any physical reality at all, a value of 0.01 volt for J seems not unreasonable. If we assume, for instance, that $N \approx 500$, we find that Inequality (31) will be satisfied in the region of the liquid helium temperatures.

In the case of actual three-dimensional crystals, N is larger by a factor of the order of magnitude of 10^{20}. Consequently, if it is permissible to use Inequality (31) also in this case, we should conclude that the validity of equations derived for $N \to \infty$ may already be doubtful at temperatures which can be obtained by adiabatic demagnetization from the region of the liquid helium temperatures.

In Fig. 1, graphs of the ratio $K_N = \chi_N/\chi_\infty$ as a function of Θ are given, for $N = 2$, 10, and 100, assuming $J > 0$.

In the same figure we also show graphs of the ratio $K_N^\circ = \chi_N^\circ/\chi_\infty$ as a function of Θ ($J > 0$), for $N = 10$ and 100, χ_N° being the atomic magnetic susceptibility of a ring macromolecule composed of N atoms subject to the Ising interaction:

$$\frac{J}{2\mu^2}\chi_N^\circ = \Theta e^{2\Theta}\frac{1 - \tanh^N\Theta}{1 + \tanh^N\Theta}. \tag{36}$$

As Kramers and Wannier (4) have shown, the partition function Z_N° of a ring macromolecule is simply

$$Z_N^\circ = \lambda_1^N + \lambda_2^N, \tag{37}$$

where λ_1 and λ_2 are given by Equations (17). Starting from Equation (37) one easily obtains Equation (36).

Also in the case of a ring macromolecule, there is a lack of uniform convergence of χ_N° to $\chi_\infty^\circ = \chi_\infty$, when N tends to infinity. However, as may be seen from Fig. 1, the deviation from the asymptotic behavior begins to be noticeable in the case of a ring macromolecule at a considerable lower temperature than in the case of a linear macromolecule.

To get some idea of how the graphs would appear in the case of $J < 0$, it is sufficient to note the following relationships.

In the case of a ring macromolecule we have:

$$K_N^\circ(-\Theta) = K_N^\circ(\Theta) \qquad \text{if } N \text{ is even,}$$
$$K_N^\circ(-\Theta) = 1/K_N^\circ(\Theta) \qquad \text{if } N \text{ is odd.}$$

In the case of a linear macromolecule we have similarly:

$$K_N(-\Theta) = 2 - K_N(\Theta) \qquad \text{if } N \text{ is even.}$$

If N is odd, no such simple relationship exists for an arbitrary Θ. However, for very low temperatures we have:

$$K_N(-|\Theta|) \approx 1/K_N(|\Theta|) \qquad \text{if } N \text{ is odd and } |\Theta| \to \infty.$$

Acknowledgments

We wish to thank the National Research Council of Canada for the support of this work. One of us (W.O.) is greatly indebted to the Lady Davis Foundation for a Fellowship.

References

1. FOKKER, A. D. Physica, 8: 109. 1941.
2. ISING, E. A. Z. Physik, 31: 253. 1925.
3. KAUFMAN, B. and ONSAGER, L. Phys. Rev. 60: 252. 1941.
4. KRAMERS, H. A. and WANNIER, G. H. Phys. Rev. 76: 1244. 1949.
5. ONSAGER, L. Phys. Rev. 65: 117. 1944.

ADAPTATION OF A CHEMICAL BALANCE FOR PRECISION WEIGHING[1]

By A. A. Hills

Abstract

Present manufacturing practices do not tend to provide for the efficient construction of balances of extreme precision. Accordingly, to satisfy the need for a balance capable of determining the difference between weights of 200 gm. nominal value to a precision of one part in 10^7, a standard chemist's balance was successfully modified without any serious difficulty.

Introduction

For weighings in metrology and other fields where an accuracy in excess of one part in 10^5 is required, satisfactory balances are becoming increasingly difficult to obtain. The decline in the master craftsmanship necessary for the construction of such balances, the delays involved in the assembly of a custom built instrument, and the tedious, extended operations required for the final adjustment make the cost disproportionately high. The effect of the disruption of schedules on the manufacturer's regular production makes him additionally reluctant to give such an instrument the full attention it deserves.

In the Metrology Section of the National Research Laboratories there was need for a balance capable of weighing in the 100 gm. to 200 gm. interval to a precision of one part in 10^7 using single Gauss exchange. In view of the above difficulties it was decided to purchase a relatively cheap chemical balance (the cost was less than $200.00) and modify it to meet the requirements.

Selection of Balance

The factors governing the selection of the original balance were:

(1) The beam was to be light and of a short rigid truss design to assure a relatively short period and a minimum departure from a linear load – sensitivity relationship.

(2) The knife-edges were to be so assembled as to be capable of precise and independent adjustment for height, parallelism, and equality of arm length.

(3) The pan suspension was to be of the "crossed" knife-edge or equivalent type, so that no turning moment about the longitudinal axis could be imparted to the beam by slight differences in the positioning of the weights on the pans.

(4) The arrestment was to locate the end planes positively to assure repetitive centering of the load on the knife-edges.

(5) The construction was to be sufficiently free from obstructions to permit ready manipulation of the weights in Gauss weighings, and to allow the modifications to be effected.

[1] *Manuscript received November 8, 1950.*
Contribution from the Metrology Section, Division of Physics, National Research Laboratories, Ottawa, Canada. Issued as N.R.C. No. 2376.

From the balances available a Sartorius analytical balance Nr. 8b was selected. Fig. 1 shows, to the left, a balance similar to the original, while on the right is the balance here described after completion.

Modifications

Mounting and Case

The equal arm balance is an extremely precise instrument, and one of the few laboratory devices that is seldom used to the full extent of its accuracy. For it to yield optimum performance it must not only be well adjusted, but must be used in a temperature-controlled, dustless, and preferably windowless room. It should be mounted on a concrete pier which is, in turn, firmly set on rock or imbedded in earth or sand reasonably free from vibration. The balance must not be subjected to irregular or unequal illumination, or air currents, and should as far as possible be shielded from the thermal disturbances caused by the operator. The need for shielding becomes obvious when it is realized that, to achieve an accuracy of one part in 10^7, the maximum change which may occur in the difference between the mean temperatures of the two halves of an aluminum beam during a Gauss weighing is 0°.008 C.

The mounting problem presented no difficulty since bedrock is readily available in the Mass Room at the Laboratories. To protect the beam an aluminum case, polished and clear lacquered on the outside and painted dull black on the inside, was assembled within the original case.

Bearing Edges and Leveling Equipment

The three planes were checked for flatness and where necessary were lapped to a precision of 0.00002 in. over the bearing surface. The surfaces defining the bearing "lines" of the knife-edges were also checked for flatness. The center flat was removed and recemented in a plane more nearly normal to the column. This plane was then brought exactly horizontal and two level vials, substituted for the original plumb bob, were adjusted to suit.

Indicator System

With the common form of indicator finger, increased sensitivity can be obtained only by raising the center of gravity of the moving system and thus increasing the arc swept by the beam for a corresponding change in load, and also, incidentally, increasing the period of swing. This procedure is inadvisable for several reasons. The knife-edge does not assume its ideal shape but, with the plane, deforms under the high pressures of loading, and may be taken as having a cylindric form, with a radius of the order of $5\mu(1)$. This causes a change in the effective lengths of the arms as the beam departs from the horizontal. It is to be noted that for a balance of this size (14 cm. beam length) the desired accuracy requires a constancy of arm lengths to within 0.014μ during a weighing. Furthermore, a large deflection puts side strain on the knife-edges at their point of attachment to the beam and may cause distortion and resulting inaccuracies. Finally, the angular deflection of the beam is not a linear function of the load inequality, and since it is desirable to use linear interpolations in

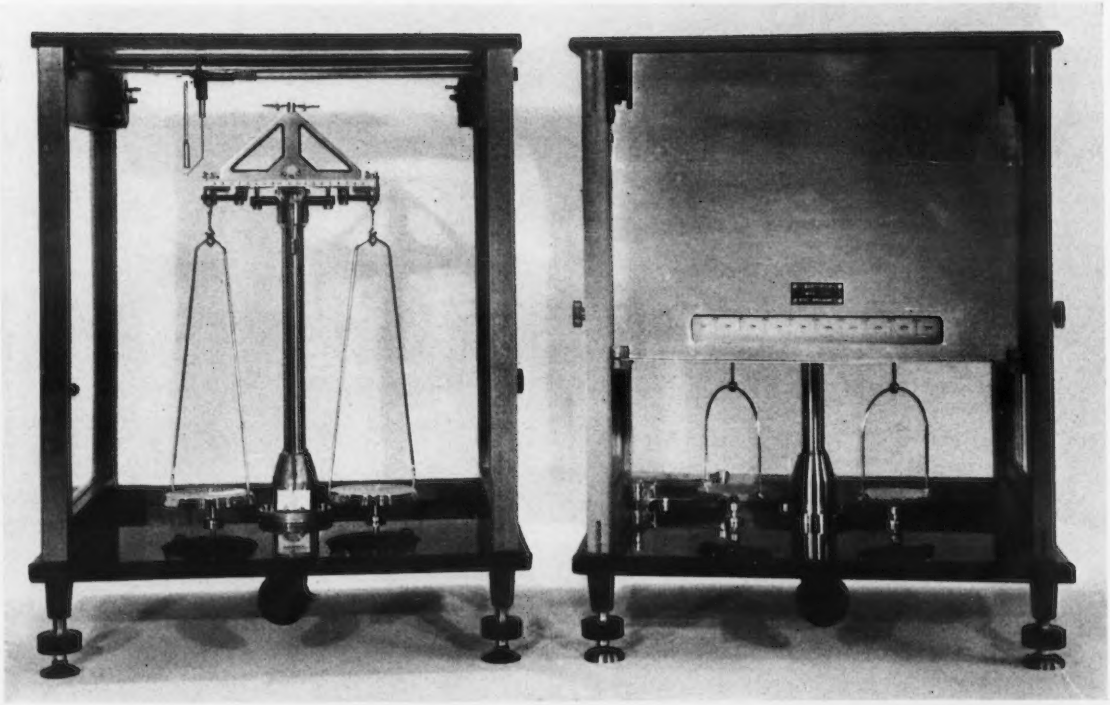

FIG. 1. *Photograph showing unmodified and modified balances. The main additions seen here are the level vials on the base plate, the modified pans, the extended scale, and a portion of the metal shielding for the beam compartment.*

sensitivity calculations it becomes necessary that the higher order terms of this deflection remain negligible.

These difficulties were overcome and a high sensitivity was obtained by using a light-beam system which, with the exception of the light source, was completely contained within the upper portion of the case. The rider system, because of the errors inherent in its use and since the modifications rendered it superfluous, was dispensed with. In its place on the beam a small aluminum bracket was mounted, carrying a very light mirror placed with its aluminized face down. (D, Fig. 2). This mirror was so positioned as to have its reflecting

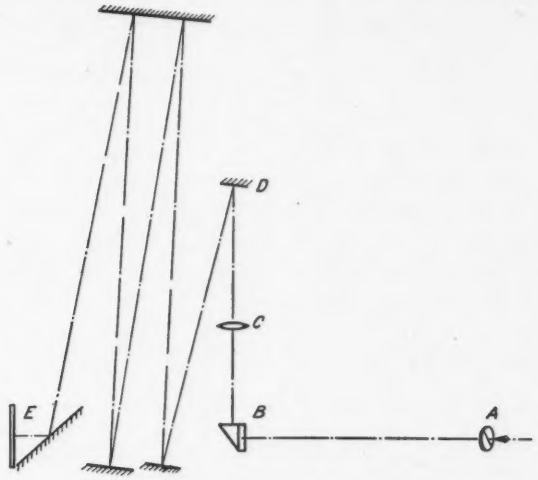

FIG. 2. *Schematic section of optic system.*

surface at the same level as the knife-edge, but inclined slightly downward toward the back. This at once practically doubled the indicated angle with respect to the beam deflection. The light was passed through a line ruled on an aluminized glass disc, A, located at the back right-hand corner of the balance, thence to a prism, B, and vertically upward through the lens, C, to the beam mirror. It was then reflected by a series of front surfaced mirrors to form an image of the line on a scale, E, mounted at the front of the case.

This system yielded the equivalent of an indicator finger of 2 metres length, and permitted a sensitivity of up to 0.01 mgm. per double millimetre division without causing an angular deflection of the beam in excess of one degree off balance point for loadings to within the nearest milligram of true balance.

Arrestment, Pans, and Adjusting Devices

The original pan arrestment rotated slightly about a vertical axis when released, and since it made contact against a surface of the pan, imparted a swinging motion to the latter. The arrestment was therefore altered to a spring-

loaded point contact type. It was also necessary, for the standardization of weights, to substitute flat pans for the existing concave style.

The balancing nuts, formerly located at the top of the beam, were removed and placed beneath the beam in a position somewhat closer to the knife-edge, to correct in some measure for the shift in the center of gravity due to the removal of the pointer. The sensitivity bob, originally fitted to slide on the pointer, was removed, and a screw adjustment type fitted to secure a more sensitive setting.

Adjustment

The degree of arm equality was determined by taking the balance point (a) at no load, and (b) from the mean of the rest points for a double weighing at 200 gm. load. From the moments about the central bearing and the sensitivity of the balance the adjustment necessary can be calculated. Since the instrument was to be used only for Gauss or Borda (substitution) weighing, the balance point would always be cancelled in the calculations, but to facilitate operation a reasonable constancy is desirable. A final figure of 0.2 mgm. shift from no load to full load was attained, representing an arm inequality of 0.07μ.

The knife-edge height was adjusted to give a decreasing sensitivity for increasing load. This is preferable in metrology work since it yields a better parts per million reading on smaller mass units.

Gould (2) defines sensitiveness as $\frac{\partial\phi}{\partial z}$, the ratio of the deflection $\partial\phi$ to the mass increment on one of the pans ∂z causing this deflection. He finds:

$$\frac{\partial\phi}{\partial z} = \frac{l}{Gs + 2a(P + Q)},$$

where:

l = the effective length of each arm of the balance,
G = the mass of the beam alone,
s = the height of the central knife-edge above the C.O.G. of the beam,
a = the distance of the central knife-edge above the plane containing two outer knife-edges,
ϕ = the beam deflection due to a mass z added to one of the pans,
P = the load on each pan (before the addition of z)
Q = the mass of one pan with suspension, etc.

For convenience in calculation, defining the sensitivity M as the inverse of the sensitiveness,

$$M = \frac{Gs + 2a(P + Q)}{l} \text{ and } \frac{\partial M}{\partial P} = \frac{2a}{l}.$$

Hence a linear sensitivity vs. load curve indicates zero beam distortion with increasing load. The slope of this curve depends on a; such a curve therefore aids in the final adjustment of the heights of the knife-edges and in the determination of the beam deflection.

In the actual adjustment of the balance the parallelism of the end knife-edges was checked by means of a special stirrup through which the load could be alternately centered on the front and rear of the knife-edges under examination. By this means, and the principles relating to arm inequality and load-sensitivity relationships just mentioned, the departures from parallelism of the knife-edges in both the horizontal and vertical planes were determined. The former was adjusted to be within 5 sec. of arc (0.2 mgm. shift for 0.25 in. of motion along the knife-edge at 100 gm. load). A sensitivity change of 5% for a similar magnitude of motion along the knife-edge was permitted.

The check was repeated to determine the effects of subsequent alterations on previous settings, and, where necessary, further adjustments were made.

Results

When finally adjusted the balance yielded a sensitivity ranging from 0.124 mgm. per double centimetre division at no load to 0.177 mgm. per double centimetre division at full load. The beam was found to deflect and change the value of "a" by 1.6μ between no load and 200 gm.

Finally the accuracy of weighing was determined by using six weights of 100 gm. nominal value. These were weighed one against the other in all possible pairs using a single Gauss exchange, and the differences determined. The results were then adjusted by the method of least squares and the probable values of the differences obtained. The results are given in Table I, where the residuals show the departure of the weighed values from the probable values.

TABLE I

COMPARISON OF WEIGHED AND MEAN SQUARE ADJUSTED DIFFERENCES FOR ALL POSSIBLE PAIRS IN A SET OF SIX 100 GM. WEIGHTS

Weight combination	Weighed difference, mgm.	Adjusted difference, mgm.	Residual, mgm.
A–B	−0.047	−0.056	0.009
A–F	+0.634	+0.636	0.002
A–X	+0.004	0.000	0.004
A–Y	−0.201	−0.200	0.001
A–Z	−0.174	−0.165	0.009
B–F	+0.691	+0.692	0.001
B–X	+0.043	+0.056	0.013
B–Y	−0.118	−0.144	0.026
B–Z	−0.112	−0.109	0.003
F–X	−0.631	−0.636	0.005
F–Y	−0.848	−0.836	0.012
F–Z	−0.797	−0.801	0.004
X–Y	−0.197	−0.200	0.003
X–Z	−0.174	−0.165	0.009
Y–Z	+0.051	+0.035	0.016

From Table I a mean residual of 0.007_8 mgm. at 100 gm. load is obtained. Since the accuracy in terms of parts per million of the load is least satisfactory at the smallest load for which the balance is to be used, it is considered that the accuracy attained in this test is a quite satisfactory indication of the performance of the balance.

Fig. 3 is a photograph of the beam compartment of the remodelled balance, with the front aluminum cover removed to show the indicator system.

Conclusions

From the satisfactory results obtained it appears that this method offers a solution to the difficulties of procuring a high precision balance. No phase of the modification or adjustment is beyond the scope of a careful and well trained instrument maker, provided he is advised of the interpretations to be placed upon the peculiarities of the behavior of the balance.

References

1. FELGENTRAEGER, W. Feine Waagen Wägungen und Gewichte. 2nd ed. Julius Springer, Berlin, 1932.
2. GLAZEBROOK, SIR R. Dictionary of applied physics. Vol. 3. MacMillan and Co., Limited, London. 1923. p. 107.

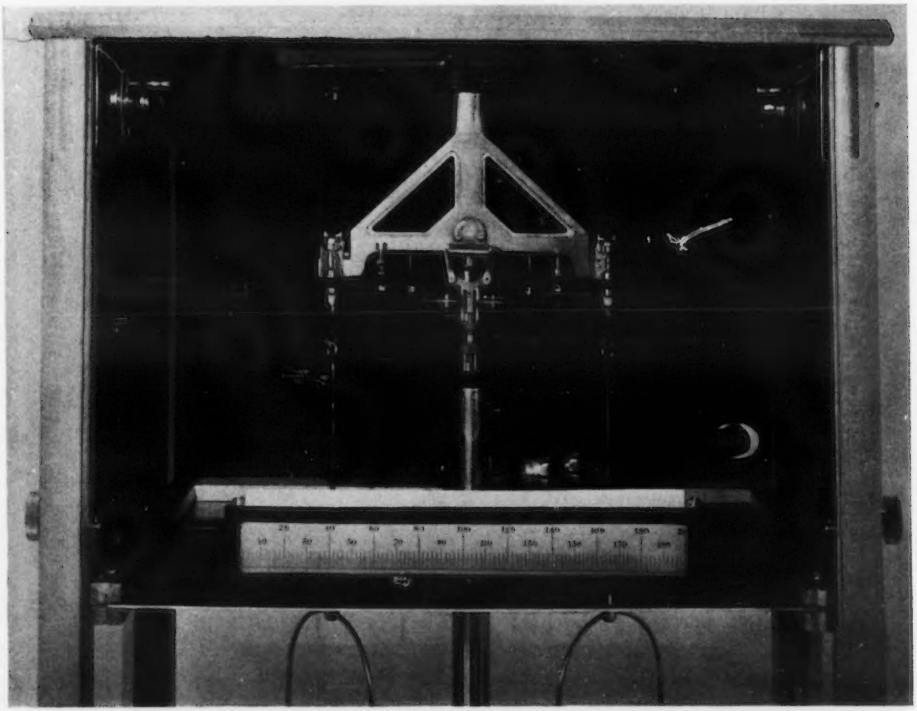

FIG. 3. *The interior of the beam compartment after alterations. The graticule, prism, and lens are carried in the tube mounted in front of the column and running to the back right-hand corner of the compartment. The beam mirror and bracket are clearly shown near the central knife-edge. The frame and bracket for the upper mirror may be seen at the top of the case, while the lower mirrors are hidden by the scale carrier.*

ABNORMAL *E* REGION IONIZATION[1]

By N. C. Gerson

Abstract

Oblique incidence radio observations on sporadic *E* reveal both the movement and geographical extent of these reflection areas. On 13 June 1949 two *Es* centers were observed by this method. The first sporadic *E* center developed rapidly until it included an area of over 10^6 km.^{2}; the second *Es* center was much smaller. The velocity of the center of mass of the first area was about SE 100 km. per hr. (in the meteorological usage; i.e., *from* the SE) and the velocity of the second, about SSE 270 km. per hr. Drift velocities in the ionosphere obtained by other investigators are of about this order of magnitude.

Introduction

An investigation of the occurrence and sweep of sporadic *E* over the North American continent was undertaken with the co-operation of radio amateurs transmitting in the frequency range 50-54 Mc. per sec. That the venture was a success, as will be seen below, may be attributed directly to the co-operativeness and enthusiasm of the radio amateurs contributing to the program.

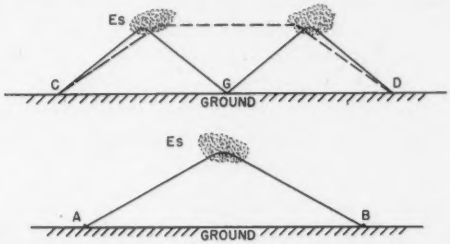

Fig. 1. *Idealized sketch indicating single and double-hop reflection from sporadic E ionization. (The propagation path shown by the dotted line has a very small degree of probability.)*

The method of reporting the existence of sporadic *E* is somewhat simple and is depicted in Fig. 1. At the radio frequencies involved, the normal distance of communication is restricted to radio line-of-sight transmission, a distance somewhat greater than the geometric line-of-sight. However, the appearance of a sporadic *E* "cloud" of sufficient refractive or scattering ability will allow communication at distances of about 650–2200 km. from the transmitter. The skip distance of 650 km. is determined by the altitude and refractive (or scattering) ability of the sporadic *E* area. The maximum distance of about 2200 km. is determined by the altitude and extent of the cloud and the earth's curvature. Thus, in Fig. 1, *A* and *B* represent, for example, two observing stations separated by about 700 km. When *Es* appears approximately over the center of the intervening region, the two stations which are not normally

[1] *Manuscript received August 18, 1950.*
Contribution from A F Cambridge Research Laboratories, Cambridge, Massachusetts, U.S.A.

in radio contact, may establish and maintain contact until the sporadic E cloud moves away.

In this connection, several types of radio wave propagation are commonly defined, indicating the number of reflections from an ionospheric layer. Thus, the case described immediately above is termed "single-hop" *Es* propagation. Another mode of propagation frequently encountered with sporadic E is double-hop, also illustrated in Fig. 1 where C and D represent the transmitting and receiving station, and G the point of reflection of the wave at the ground. It should be realized that the ideal portrayal of double-hop ionospheric propagation may be complicated by the absence of the ground reflection, as shown by the dotted path. Also, the effect of the vertical boundaries of the sporadic E cloud has not been considered in either case. In any event, the subsequent analysis is based upon these simple models of single-hop and double-hop transmission. It is, of course, possible to have triple-hop *Es* but such occurrences are rarely observed.

Screening the Data

Before the data may be utilized, they must be carefully examined to ensure that the reported radio contacts may be attributed to sporadic E reflection. Thus, any contacts by means of (*a*) the direct ground wave, (*b*) tropospheric refracted waves, (*c*) auroral interacted waves, and (*d*) F_2 ionospheric layer reflected waves, must be eliminated from the reported information. At a frequency of about 50 Mc. per sec., the range of the direct ground wave is limited by radio line-of-sight to about 80 km. Thus any observations inadvertently containing radio contacts which lie within this distance are quickly discerned and dismissed from the analysis.

Tropospheric refracted waves may extend the range of contact to and occasionally even well beyond the skip distance of 650 km. Refraction of this type arises during the existence of meteorological conditions conducive to the formation of ducts for the frequency concerned. The proper temperature and moisture lapse rates and inversions form a "leaky wave guide" which may allow superrefraction to extend the normal range of contact considerably. In temperate latitudes this effect occurs mainly during the summer and affects the propagation of the smaller wave lengths much more than it does the propagation of six meter waves. Depending upon the strength and thickness of the duct, there is a limiting frequency below which the duct cannot trap the wave energy. While tropospheric refraction of 50 Mc. per sec. transmission is not common, the existence of this effect may be determined by examining the meteorological maps and the radiosonde soundings over the geographic region in question at the time of the reports.

Auroral interacted waves are reported on many occasions, when visible aurora is present, by observers in middle latitudes not normally in contact with each other. If the observers at both the receiving and transmitting points have directive antenna arrays, it is found that when both antennas are directed

northward, or more specifically, towards the visible aurora, these observers may establish radio contact. In general the signal received during such a transmission fades rapidly and is peculiarly garbled, giving the impression that the refraction or scattered screen is in violent motion. When reporting, the radio amateurs themselves differentiate between contacts made by auroral interaction and usual sporadic E reflection. Radio contacts at a frequency of 50 Mc. per sec. by means of F_2 ionospheric layer refraction are somewhat rare. Contacts by this mode occur only when the normal layer is ionized to a much greater extent than usual. However, the occurrence of such unusual electron density in the F_2 region may be discerned by examining the ionospheric records obtained at the regular vertical incidence ionospheric stations.

The observational data are sent by each amateur to a central group which carefully screens the data to ensure that only observations which may be attributed to sporadic E are used in the analysis. In some cases other modes of transmission are inadvertently included with the primary data; these are eliminated according to the manner outlined above.

After the screening process is completed, the data are plotted on outline maps of North America. As is obvious from Fig. 1, only the midpoint of the great circle path between the two observers need be plotted with single-hop transmissions. With double-hop transmission the midpoint of each half of the great circle path is plotted. To differentiate between the two modes of propagation, the midpoint of single-hop *Es* is indicated by a dot; with double-hop *Es* an "*x*" indicates each of the two midpoints. (See Figs. 2-8.) The agreement between the points plotted as single-hop and double-hop is gratifying and strengthens belief in the accuracy of the results.

Description of Results

During June 1949 somewhat heavy sporadic E activity was reported almost daily from the vertical incidence ionospheric stations over North America, and was observed also by the co-operative amateur network. This paper will describe results obtained on 13 June during the period 0200–0800 GMT, when a very large number of *Es* reports was made by the observers. The screened data were plotted on the maps shown in Figs. 2-8. Each map contains all observations during the 60 min. period centering on the GMT hour indicated.

Two centers of action may be noticed at 0200 GMT; one rather small and located near central Arizona, the other somewhat larger and centered about Kansas. The smaller *Es* area moved from the SSE at an average speed of about 270 km. per hr. during the next two hours, after which it was centered over northeastern Nevada. During the following hour this sporadic E center remained almost stationary and after 0500 GMT it apparently dissipated rapidly inasmuch as no observations were subsequently reported. The almost total cessation of movement during the dissipative period seems to be a characteristic of the *Es* as thus far observed.

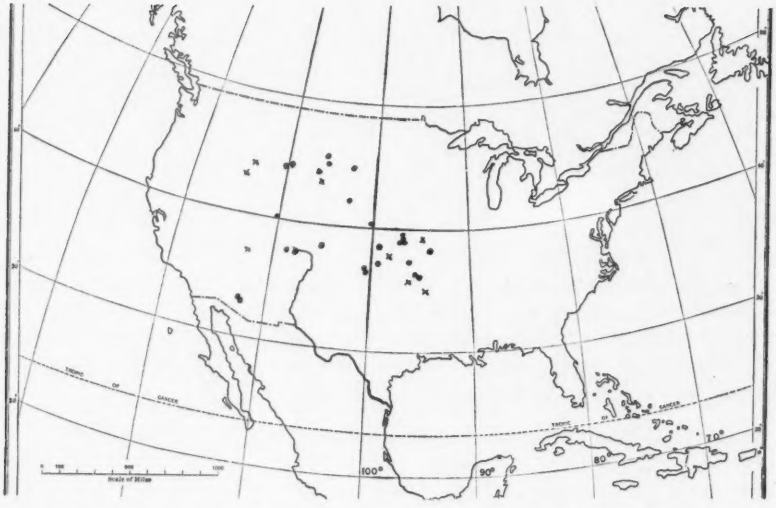

FIG. 2. *Plot of sporadic E reflections during the hour centering on 0200, GMT, 13 June 1949.*

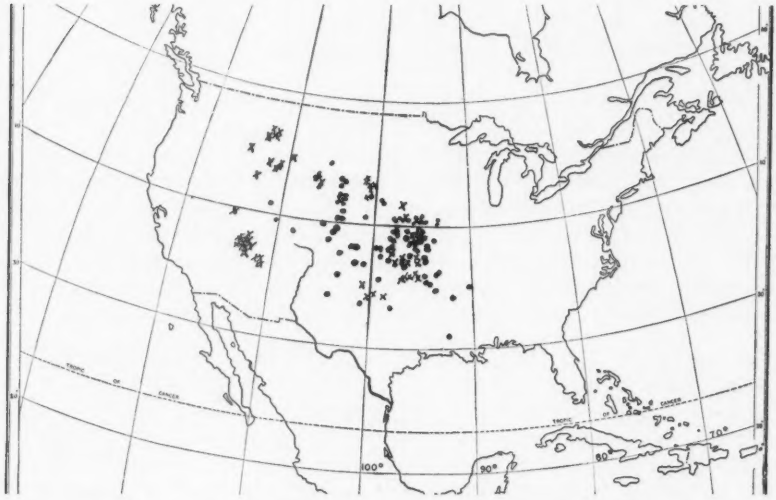

FIG. 3. *Plot of sporadic E reflections during the hour centering on 0300, GMT, 13 June 1949.*

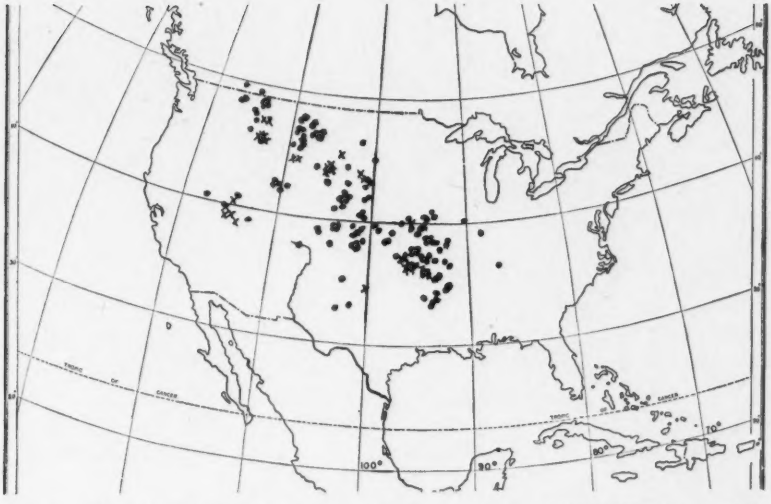

FIG. 4. *Plot of sporadic E reflections during the hour centering on 0400, GMT, 13 June 1949.*

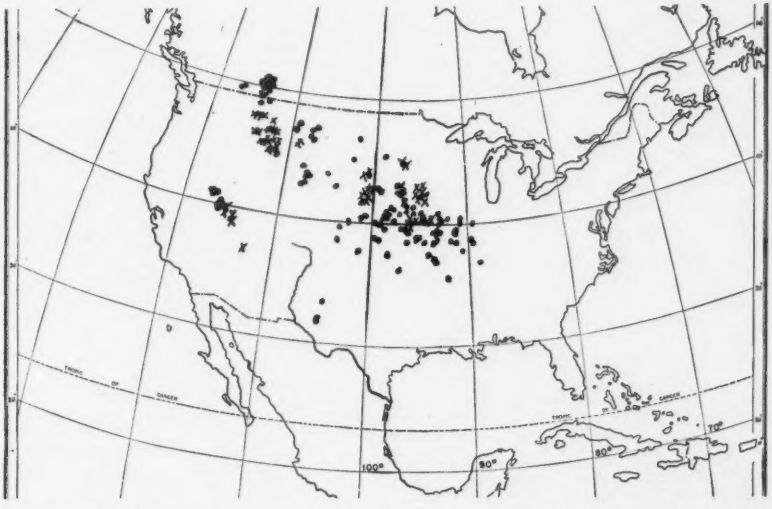

FIG. 5. *Plot of sporadic E reflections during the hour centering on 0500, GMT, 13 June 1949.*

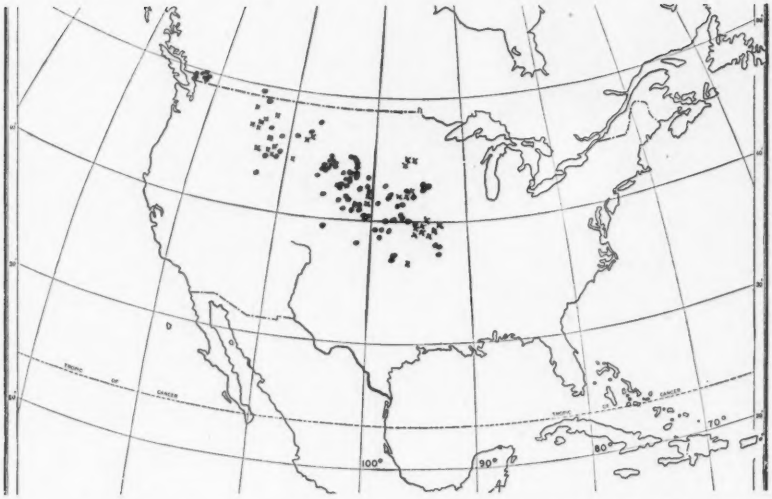

FIG. 6. *Plot of sporadic E reflections during the hour centering on 0600, GMT, 13 June 1949.*

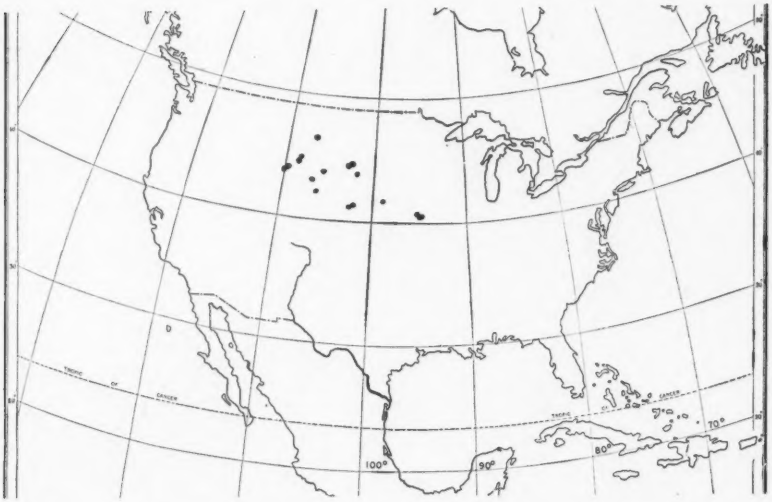

FIG. 7. *Plot of sporadic E reflections during the hour centering on 0700, GMT, 13 June 1949.*

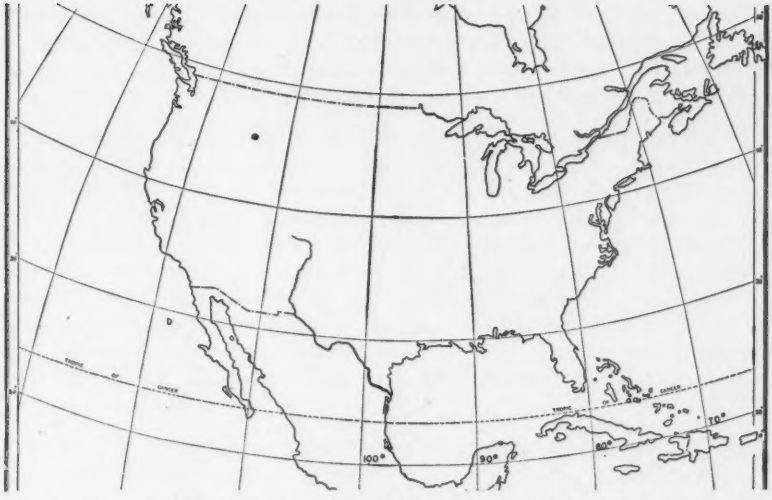

FIG. 8. *Plot of sporadic E reflections during the hour centering on 0800, GMT, 13 June 1949*

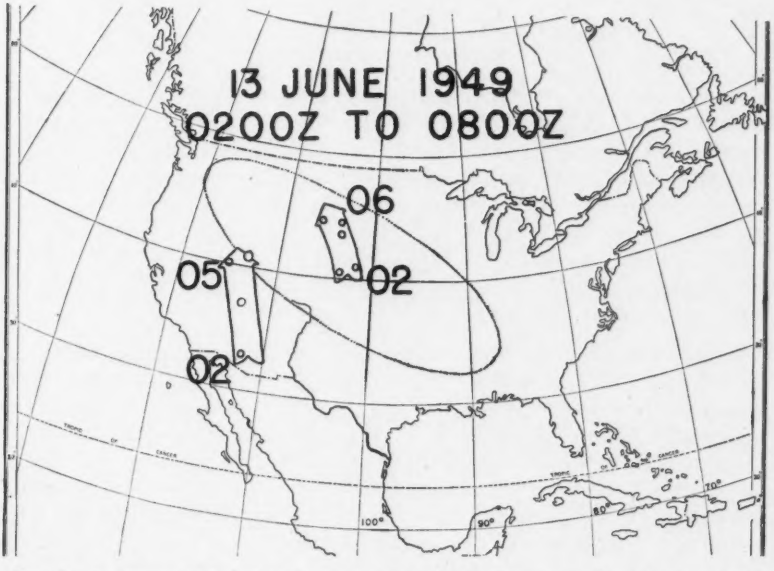

FIG. 9. *Summary sketch showing the movement of sporadic E areas over North America during the interval 0200-0800 GMT, 13 June 1949.*

The second area of sporadic E appeared to act as a pulsating ellipse—one which originally of moderate size expanded (unequally) to much larger dimensions and then contracted to insignificance. In general, the "center of mass" (considering each plotted point as having unit mass) of this region moved from the SE at a velocity of about 100 km. per hr.

In the case of the larger *Es* area reported above, the mean velocity of the center of mass may be low and subject to some doubt. This doubt arises from the possibility that the expansion of the ellipse may have extended further into southwestern Canada; however, no reports from amateur radio operators are available for that geographic location. The somewhat abrupt deceleration of the northerly expansion may be real; contrarily, it may merely indicate that the paucity of observers in southwestern Canada did not permit the true northerly limits of the reflection area to be observed. The rapid and total disappearance of the *Es* after its apparent deceleration is very marked, as is strikingly shown by the nearly complete absence of *Es* during the hour 0800 GMT.

A summary of the movements of the center of mass of each sporadic E region is shown in Fig. 9. Also shown is the maximum observed extension of the elliptic reflection area, which had a major axis of about 3000 km. and a minor axis of about 1200 km. The fact that the direction of motion of this area does not coincide with either axis should be noted.

Discussion of Results

Drift or wind velocities determined in the ionospheric regions by observations on some type of ionospheric irregularity have been reported previously by other investigators. Employing a technique similar to that described in this paper Ferrell (5) found speeds of 290–380 km. per hr. from the east over the United States. Later results (6) show velocities of about 360 km. per hr. also from the east in January and about 170 km. per hr. from the SES in July. With the same technique, Gerson (7, 8) found velocities of SSE 125 km. per hr. (in the meteorological sense; i.e., from the SSE) in May. The above results are of the same magnitude as those obtained in this investigation.

Velocities of winds in the ionosphere have been obtained also by noting the time of appearance of sporadic E reflections at two vertical incidence ionospheric stations somewhat closely spaced. With a distance of about 60 km. between the stations, Mimno (11) found that an E region cloud required about one minute to pass from one station to the second. In this case, the velocity was about E 3600 km. per hr. Dieminger, Goubau, and Zenneck (3) reported a speed of about 3600 km. per hr. over Germany. Eyfrig (4) reported wind velocities or components of velocity from the north at speeds of 140–1152 km. per hr. For F_2 region motions, Beynon (2) reported a value of 430 km. per hr. from the east. Mitra (12) found speeds of 72–390 km. per hr. at a height of 70–115 km. over England.

Meek (10) undertook measurements of the speed of sporadic E clouds over Baker Lake, N.W.T, Canada, and obtained values of 300–700 km. per hr. Meek's analysis was essentially a single station determination. The drift speed was deduced by considering the rate of change in slant range of an ionospheric "cloud" which when in the zenith had the same altitude as the E layer. This phenomenon was interpreted as an *Es* area moving from a distance towards the station zenith, then moving away in the opposite direction. No information could be obtained regarding the direction of motion.

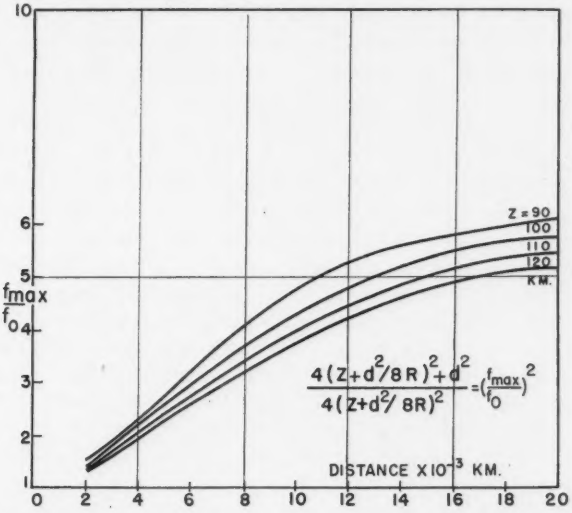

FIG. 10. *Graph of the function* $(f_{max}/f_0)^2 = (a^2 + d^2)/a^2$, *where* $a = 2(z + d^2/8R)$.

Using the three-station technique for the determination of both direction and velocity of ionospheric drifts, Krautkrämer (9) found the directions of motion in the E layer mainly from the sector SSE to WSW, with movements generally from the western sectors. The most frequently reported speed was about 500 km. per hr. over Germany. In general, however, he found speeds ranging from about 100–1400 km. per hr.

Perhaps a word of caution regarding the intercomparison of wind velocities should be made. First, it should be clearly recognized that all wind velocities obtained are based upon a fundamental assumption: that any radial velocity component away from the earth is zero or essentially so. If marked subsidence effects or other vertical motions in the ionic density were to occur, the apparent magnitude and direction of the determined winds may be seriously in error.

A possible explanation of the sudden appearance of sporadic E over a given locality may be obtained by reference to Fig. 10. The curves on this diagram

were obtained from the formula originally derived by Appleton (1):

$$(f_{max}/f_0)^2 = (a^2 + d^2)/a^2, \tag{1}$$

where

$$a = 2(z + d^2/8R).$$

In the above equation f_{max} is the maximum value of the radio frequency which may be employed for communication between two points separated by the distance d located on the surface of an earth of radius R. The symbol f_0 indicates the vertical incidence critical (or penetration) frequency of the ionized region located at an altitude z. This formula was derived for a *thin* ionospheric layer, neglecting the effect of the geomagnetic field as well as the effect of collision frequency.

If there exists a cloud of sporadic E ionization of given electron density (so that f_0 is a constant) and if a single radio frequency f_{max} is employed for oblique incidence transmissions, then the left side of Equation (1) is constant. A suitable ratio may be $f_{max}/f_0 = 5.0$.

Assume that the ionized cloud is originally at an altitude of 120 km. and then sinks to 90 km. If the distance between the two stations concerned is about 1100 km. it is found that in so far as the observers are concerned, the *Es* cloud becomes evident as soon as it reaches an altitude of about 95 km. When the cloud is at higher levels, these two amateurs cannot establish contact and they cannot report the existence of the *Es* as long as the frequency ratio defined above is true. The existence of a bodily lowering of a region capable of refracting or scattering 50 Mc. per sec. radio waves at oblique incidence has been reported from probings made at vertical incidence ionospheric stations. The above explanation attributing the sudden appearance or disappearance of a sporadic E area (as observed between two fixed points at a given frequency) to a radial motion towards or away from the earth is therefore possible. However, the vertical motions of an *Es* area only change the geographic locations from which the radio observers may contact each other; the midpoint of the path remains unchanged.

It should also be noted that some observational bias is inherent in the reported data because of the operating habits of the observers. The geographical distribution of the amateurs operating at 50 Mc. per sec. is not well distributed over the continent. For example, a serious dearth of observers exists in western and central Canada both in the south and the north. Obviously, also, the hours of operation influence the data.

It may be thought that because of the absence of obstacles at the altitudes concerned, wind velocities at 100 km. determined anywhere over the globe would be closely similar. However, it is conceivable that an atmospheric heat source arising through insolation may exist somewhat below 100 km. In this case, a diurnal and seasonal effect in the wind velocity may occur over any particular geographic point, and, if unequal insolation occurs, the wind velocities may in fact differ at different localities. Thus, some reason exists for not believing a priori that winds 100 km. over Ottawa, for example, are directly comparable with motions at the same altitude but over Calcutta.

Acknowledgments

Appreciation is expressed to the amateur radio fraternity for providing the fundamental reports upon which this study is based, to the staff of Radio Magazines, Inc., under Mr. O. P. Ferrell for screening the data, and to F. J. Crowley for plotting.

References

1. APPLETON, E. V. Proc. Cambridge Phil. Soc. 23: 151. 1926.
2. BEYNON, W. J. G. Nature, 162: 887. 1948.
3. DIEMINGER, W., GOUBAU, G., and ZENNECK, J. Hochfrequenztechnik und Elektroakustik, 44: 2. 1934.
4. EYFRIG, R. Hochfrequenztechnik und Elektroakustik 56: 161. 1940.
5. FERRELL, O. P. Proc. I.R.E. 35: 493. 1947.
6. FERRELL, O. P. Proc. I.R.E. 36: 879. 1948.
7. GERSON, N. C. CQ, 6: 17. 1950.
8. GERSON, N. C. Nature, 166: 316. 1950.
9. KRAUTKRÄMER, K. Deutsche Luftfahrtforschung, Forsc. No. 1761. 1943.
10. MEEK, J. H. J. Geophys. Research, 54: 339. 1949.
11. MIMNO, H. R. Revs. Modern Phys. 9: 1. 1937.
12. MITRA, S. N. Proc. I.E.E. III, 96: 441. 1949.

CANADIAN JOURNAL OF PHYSICS

Notice to Contributors

GENERAL: Manuscripts should be typewritten, double spaced, and the **original and one extra copy** submitted. Style, arrangement, spelling, and abbreviations should conform to the usage of this Journal. Names of all simple compounds, rather than their formulas, should be used in the text. Greek letters or unusual signs should be written plainly or explained by marginal notes. Superscripts and subscripts must be legible and carefully placed. Manuscripts should be carefully checked before being submitted, to reduce the need for changes after the type has been set. If authors require changes to be made after the type is set, they will be charged for changes that are considered to be excessive. **All pages, whether text, figures, or tables, should be numbered.**

ABSTRACT: **An abstract of not more than about 200 words, indicating the scope of the work and the principal findings, is required.**

ILLUSTRATIONS:

(i) *Line Drawings:* All lines should be of sufficient thickness to reproduce well. Drawings should be carefully made with India ink on white drawing paper, blue tracing linen, or co-ordinate paper **ruled in blue only;** any co-ordinate lines that are to appear in the reproduction should be ruled in black ink. Paper ruled in **green, yellow, or red should not be used** unless it is desired to have all the co-ordinate lines show. Lettering and numerals should be neatly done in India ink preferably with a stencil (**do not use typewriting**) and be of such size that they will be legible and not less than one millimeter in height when reproduced in a cut three inches wide. All experimental points should be carefully drawn with instruments. Illustrations need not be more than two or three times the size of the desired reproduction, but the ratio of height to width should conform with that of the type page. **The original drawings and one set of small but clear photographic copies are to be submitted.**

(ii) *Photographs:* Prints should be made on glossy paper, with strong contrasts; they should be trimmed to remove all extraneous material so that essential features only are shown. Photographs should be submitted **in duplicate;** if they are to be reproduced in groups, one set should be so arranged and mounted on cardboard with rubber cement; the duplicate set should be unmounted.

(iii) *General:* **The author's name, title of paper, and figure number should be written in the lower left hand corner (outside the illustration proper) of the sheets on which the illustrations appear.** Captions should not be written on the illustrations, but typed on a separate page of the manuscript. All figures (including each figure of the plates) should be numbered consecutively from 1 up (arabic numerals). **Each figure should be referred to in the text.** If authors desire to alter a cut, they will be charged for the new cut.

TABLES: Each table should be typed on a separate sheet. Titles should be given for all tables, which should be numbered in Roman numerals. Column heads should be brief and textual matter in tables confined to a minimum. **Each table should be referred to in the text.**

REFERENCES: **These should be listed alphabetically by authors' names, numbered in that order, and placed at the end of the paper.** The form of literature citation should be that used in this Journal. **Titles of papers should not be given.** The first page only of the references cited should be given. **All citations should be checked with the original articles.** Each citation should be referred to in the text by means of the key number.

REPRINTS: A total of 50 reprints of each paper, without covers, are supplied free to the authors. Additional reprints will be supplied according to a prescribed schedule of charges. On request, covers can be supplied at cost.

Approximate charges for reprints may be calculated from the number of printed pages, obtained by multiplying by 0.6 the number of manuscript pages (double-spaced typewritten sheets, 8½ in. by 11 in.) and making allowance for space occupied by line drawings and half-tones (not inserts). The cost per page is tabulated at the back of the reprint request form sent with the galley.

Manuscripts should be addressed: *Canadian Journal of Physics,*
National Research Council,
Ottawa, Canada.

Contents

	Page
On the Penetrating Showers of Cosmic Rays—*André G. Voisin*	205
Selective Reflection from the Vapors of the Alkali Metals—*A. C. Lauriston and H. L. Welsh*	217
The Sudden Increase in Cosmic Ray Intensity, November 19, 1949—*D. C. Rose*	227
Statistics of a Linear Paramagnetic Macromolecule — *W. Opechowski and J. M. Bryan*	236
Adaptation of a Chemical Balance for Precision Weighing—*A. A. Hills*	245
Abnormal *E* Region Ionization—*N. C. Gerson*	251